RSC Advances

ROYAL SOCIETY OF CHEMISTRY

www.rsc.org/advances

PEG Functionalized Selenium Nanoparticles as a Carrier of Crocin to Achieve Anticancer Synergism

Thottumugathu Ancil Mary[2†], Krishnamurthy Shanthi[2†], Vimala Karuppaiya[1†] and Kannan Soundarapandian*[1]

† These authors contributed equally to this manuscript.

[1] Proteomics and Molecular Cell Physiology Laboratory, Department of Zoology, Periyar University, Salem-636 011, Tamil Nadu, India

[2] Department of Zoology, Bharathiar University, Coimbatore-641 046, Tamil Nadu, India.

* Corresponding author at:

Department of Zoology,

Periyar University,

Salem-636 011,

Tamil Nadu,

India.

Tel.: *0427-2345766, 2345520*

E-mail address: skperiyaruniv@gmail.com (S. Kannan).

1. Introduction

Cancer is one of the most feared diseases globally and there has been a sustained rise in its incidence in both developing and developed countries. It is one of the major non-communicable diseases posing a threat to world health. Despite the growing therapeutic options for patients with cancer, their efficacy is time-limited and also their curable ability is limited.[1] The current cancer treatments often kill healthy cells and thus show significant toxicity and unavoidable side effects.[2] Therefore, the discovery of novel, selective, efficient, and safe drugs for cancer chemotherapy remains an urgency and high priority for medicinal research.[3] Currently, nanoparticle-based drugs are emerging as an important class of therapeutics.[4] The most promising aspects of utilizing nanoparticles as therapeutics are their potential to localize (or be targeted) in a specific manner to the site of disease and reduce or eliminate the possible numerous untoward side effects. The nanometric size of these materials precludes them from being readily cleared through the kidneys, thereby extending circulation in the blood pool depending on their surface-functionalization characteristics.[5] Also, when considering novel cancer treatments, blood vessels in many tumor types are irregular in shape, dilated, leaky, and can present fenestrations in endothelial cells. Due to the altered anatomy of tumor vessels, nanosized particles can easily extravasate from the blood pool into tumor tissues and be retained due to poor lymphatic drainage. This phenomenon of selective accumulation of nanosized particles near tumor tissues is termed the enhanced permeability and retention (or EPR) effect.[6, 7] Additionally, nanoparticles have high surface area-to-volume ratios, yielding high loading capacities. Thus, nanoparticles can be loaded with therapeutic drugs and imaging agents; they may also be surface-functionalized with targeting ligands and cloaking agents like poly(ethyleneglycol) (PEG), with the goal of reducing systemic toxicity.

A number of nanosystems with different structure and compositions, such as metals, polymers, oxides, and semi-conductors, have been designed and prepared to carry anticancer drugs .[8,9,10,11] Among these nanomaterials, selenium nanoparticles (SeNPs) have garnered a great deal of attention as potential cancer therapeutic agents and drugs carriers. [12,13,14,15,16] Selenium (Se) is an essential trace element with important physiological functions and extensive pharmacological actions. It is a structural component of the active centre of many antioxidant enzymes and functional proteins.[17] Se NPs possess potent effects both on scavenging various free radicals and on protecting DNA from oxidation damage *in vitro*. Se NPs could efficiently increase the activity of selenoenzymes, including glutathione peroxidase, phospholipid hydroperoxide glutathione peroxidase thioredoxin reductase and deiodinase .[18] Cellular Se plays an important role in the reduction of oxidative stress in the body. [19] It also regulates the function of the thyroid gland and helps in the proper functioning of the immune system. [20] It plays an important role to prevent various diseases, such as diabetes, hypercholesterolemia,[21] cardiovascular disease. [22, 23] Many studies have shown that the supplementation of Se could prevent cancer and reduce cancer incidence. [24,25,26] Moreover, recent studies have indicated that Se NPs express important anticancer activity by inhibiting the growth or triggering the apoptosis of different types of cancer cells containing human hepatocyte cells (HepG2), [27] human breast-cancer cells (MCF-7, MDA-MB-231), [28] human melanoma cells (A375), [29] human cervical carcinoma cells (HeLa). [30] Despite the cytotoxicity toward cancer cell lines, Se NPs could enhance the cell viability and minimize the DNA damage caused by UV exposure on human lymphocytes. [31] Although clinical trials with Se are currently limited to cancer chemoprevention, recent evidence strongly showed the potential for utilization of Se in a new way, to overt cancer through a combination with well-established chemotherapeutic and hormonal agents. Many

studies showed that Se could sensitize cancer cells to conventionally used anticancer drugs. [32,33] Over the past decade, SeNPs have attracted increasing attention because of their antioxidant activities and low toxicity. [34,35] Compared to other nanoparticles that are currently most often studied, such as gold nanoparticles, SeNPs are superior, because Se is degradable *in vivo.* Degraded Se can be used as a nutrient for many kinds of normal cells or as an antiproliferative agent for many kinds of cancer cells. [36] Abundant evidence supports the better biocompatibility, bioefficacy and lower toxicity of SeNPs by comparing with inorganic and organic selenocompounds. [37] In addition, SeNPs, by nature, display desired biological activities and can be used as drug carriers as well. In this study, we report the use of SeNPs as carriers of crocin to enhance their anticancer outcome.

Crocin, a major active product of saffron (dried stigmas of *Crocus sativus*), has many therapeutic properties such as antitumoral, [38,39] antioxidant, [40] anxiolytic, [41,42] neuronal protective,[43] anti-ischemic [44] and protective against DNA damage [45] activities. Crocin are also effective agents as antidepressant, anticonvulsant, memory enhancer and sedative in treatment of central nervous system disorders.[46] Owing to the therapeutic potential of both SeNPs and crocin, we look forward to design a synergistic system by conjugating crocin to the surface of the SeNPs, which could enhance the cure rate and lower their toxicity. By altering the surface chemistry of SeNPs using PEG, crocin could be conjugated to the nanoparticles, and this drug delivery system can be utilized to target cancer. Herein, we describe the synthesis of PEG functionalized SeNPs (PEG-SeNPs) and its use as a cancer-targeted drug delivery system for crocin to achieve enhanced anticancer efficacy against lung cancer. The *in vivo* anticancer activity of crocin conjugated PEG-SeNPs and the underlying molecular mechanisms were also investigated in this study.

2. Experimental

2.1. Materials

Human normal lung epithelial cell lines L-132 and lung cancer A549 cell were procured from National Centre for Cell Science (Pune, India). Certified dried Saffron stigma sample were purchased from Coimbatore, Tamilnadu. Sodium selenite (Na_2SeO_3), poly(ethylene glycol) (200k) (PEG), 3-(4,5-dimethylthiazolyl-2)-2,5-diphenyltetrazolium bromide (MTT), 4′-6-diamidino-2-phenylindole (DAPI), *acridine orange*/*ethidium bromide (*Ao/EtBr), Dulbecco's Modified Eagles medium (DMEM) were purchased from Sigma–Aldrich (Bangalore). Analytical grade reagents were purchased from Sigma–Aldrich (Bangalore). All the samples were prepared in Milli-Q water.

2.2. Extraction of crocins from saffron stigmas

Crocin was isolated from saffron by previously described method. [47] Saffron stigmas powders (10 g) were suspended in 25 mL ethanol (80%) at 0°C and shaked by vortex for 2 min. After centrifugation at 4000 rpm for 10 min the supernatant was separated. 25 ml of ethanol (80%) was added to sediment and extraction was repeated again. This step was repeated 6 other times. The total volume of solvent consumption for 10 g saffron stigmas in extraction process was 200 mL (8×25 mL). The resulting solution was kept in a thick walled glass container at -5°C for 24 days in darkness. The container was sealed in this period. The obtained crystals were separated from solution and washed with acetone to remove remaining water. The yielded amount of crystals was 1.7 g. In the next step, the obtained crystals were dissolved in 120 mL ethanol (80%) and kept at -5°C in darkness for 20 extra days for re-crystallization. The final amount of yielded crystals was 1.02 g.

2.3. HPLC Analysis

For HPLC analysis, we used a Varian 9012 liquid chromatographic system equipped with a Varian 9050 UV detector (Walnut Creek, CA). The separations were carried out on a Phenomenex Lichrosphere 5 RP C18 column (250×4.6 mm, 5μm) (Torrance, CA). The precolumn was a Phenomenex C18 column (30 × 4 mm). The detector was set at 442 nm with a spectral acquisition rate of 1.25 scans/s. For the mobile phase, solvent A (methanol) and solvent B [1% (v/v) aqueous acetic acid in water] were used. The mixing of the gradient solvent eluting system was as follows: initial 30% A and 70% B; 0–5 min, linear change to 40% A; 5–10 min, change to 55% A; 10–25 min, change to 68% A; 25–27 min, change to 90% A; 27–30 min, 90% A; 30–33 min, change to 30% A; 33–40min, 30% A. The flow rate of the mobile phase was 0.8 ml/min, and the injection volume was 20 μl. All solutions were filtered through a 0.2-μm hydrophilic polypropylene membrane (Merck Millipore, Billerica, MA) before use. Separation was accomplished at 25 ^{0}C. Five different concentrations of crocin solutions were prepared to determine the calibration curve. The calibration curve was constructed with crocin content versus peak area (y = 0.0002x + 1.0422; R2 = 0.9993; linear range: 0.01–0.2 mg/ml). The content of crocin was calculated using the standard curve of crocin, and determinations were repeated 3 times.

2.4. Preparation of PEG- SeNPs

PEG- SeNPs was synthesized using a previously reported method with slight modification.[48] A stock solution of 5 mM sodium selenite (Na_2SeO_3) was prepared by dissolving 8.7 mg of Na_2SeO_3 powder in 10 mL of Milli-Q water. A 5 mL aliquot of Na_2SeO_3 stock solution was mixed with 10 mL PEG200 solution at 210°C–220°C for 15–20 minutes, under magnetic stirring. The product was then mixed with water in a 1:1 ratio. The solution was

centrifuged at 10,000 rpm for 10 minutes and then washed with Milli-Q water five times to remove excess PEG. The obtained products were characterized by various spectroscopic methods.

2.5. Preparation of crocin conjugated PEG- SeNPs

Crocin was conjugated onto PEG- SeNPs by a previously reported method with slight modification. [49] A 5 mL aliquot of PEG- SeNPs was mixed with 5 mL of 32.5 mg/mL crocin solution. The mixture was reconstituted to a final volume of 25 mL with Milli-Q water. Then the mixed solution was stirred for 24 h at room temperature. Excess crocin were removed by dialysis against Milli-Q water overnight. Se concentration was determined by ICP-AES analysis.

The drug loading efficacy was calculated by two ways, first based on indirect method by estimating the crocin content of the supernatant and second based on direct estimation of the crocin content present in the pellet obtained after centrifugation. The drug concentration in supernatant and redispersed pellets was determined by measurements of its UV absorbance at 470 nm using UV/visible spectroscopy and the percentage loading of crocin onto nanoparticles were estimated by the following formula.

$$Loading\ efficiency = \frac{wo}{w} X\ 100$$

where, Wo is the weight of crocin conjugated on the PEG-SeNPs, W is the weight of PEG-SeNPs.

2.6. *In vitro* drug release of crocin conjugated PEG-SeNPs

Two copies of crocin conjugated PEG- SeNPs (10 mg) were respectively suspended in 10 ml PBS solution at pH 5.3 and pH 7.4 with constantly shaking in dark tubes at 37^0 C. At specific intervals, a certain volume of buffer was taken out from tubes and same volume of fresh buffer

was replaced. For the measurement of released crocin concentration, the absorbance of the release medium at 475 nm was recorded on a Shimadzu UV-*vis* absorption spectrophotometer.

2.7. Cell Viability Assay

Cell viability was determined by measuring the ability of cells to transform MTT to a purple formazandye.[50] Cells were seeded in 96-well tissue culture plates at 2.5 x 10^3 cells/ well for 24 h. The cells were then incubated with crocin conjugated PEG- SeNPs at different concentrations for different periods of time. After treatment, 20 µL/well of MTT solution (5 mg/mL phosphate buffered saline) was added to the well and incubated for another 5 h. To dissolve the formazan salt formed, the medium was aspirated and replaced with 150µL/well DMSO. The cell growth condition was reflected by the color intensity of the formazan solution. Absorbance at 570 nm was taken on a 96-well microplate reader (MD VERSA max).

2.8. Synergy analysis

Isobologram method was conducted to analyze the synergistic effect between PEG-SeNPs and crocin. Briefly, line segment between the IC_{50} value of PEG-SeNPs and crocin on the x- and y- axes respectively represented the additive line. The data point near or on the additive line represented an additive treatment effect, while the data point below or above the additive line remarked the synergism or antagonism respectively. In addition, the extent of synergism or antagonism was evaluated by combination index (CI). CI value of 1 meant an additive effect between two drugs, while CI value < 1 represents synergism, CI value > 1 indicates antagonism. The extent of CI value below or above 1 is positively related to the extent of synergism and antagonism respectively.

2.9. Fluorescence microscopic studies

2.9.1. HOECHST 33342 staining

The selected cancer cells were seeded in 6 well plates and maintained at 37 ^{0}C with 5% CO_2 in a humidified CO_2 incubator for 48 h. Subsequently, the cells were treated with crocin conjugated PEG- SeNPs with their IC_{50} concentrations obtained after incubation for 24 h, and 48 h. At the indicated times, the medium was removed gently and the cells were washed twice with phosphate buffered saline(PBS), fixed in 4% paraformaldehyde for 20 min, re-washed, and stained with HOECHST 33342 (10µg/mL) at 37 ^{0}C for 20 min in the dark. Stains were then washed with methanol followed by PBS, and the plate was immediately observed in blue channel fluorescence with fluorescent microscopy (Nikon Eclipse, Inc., Japan).

2.9.2. AO/EtBr staining

1mL of a dye mixture (100 mg/mL acridine orange (AO) and 100 mg/mL ethidium bromide (EtBr), in distilled water) was directly stained with crocin conjugated PEG- SeNPs treated cells grown on clean microscope cover slips. After staining the cancer cells were washed with PBS (pH 7.2) and incubated for 1 min, the cells were then visualized under fluorescence microscope (Nikon Eclipse, Inc., Japan) at 400 × magnifications with an excitation filter at 480 nm.

2.9.3. Rhodamine 123 staining

A549 cells were seeded in 6 well plates (1×10^5cells/well) and allowed to grow for a day before exposed to IC_{50} concentrations of crocin conjugated PEG- SeNPs. After the specific time intervals (24, and 48), the cells were fixed in 4% para-formaldehyde, washed twice with PBS, and exposed to the Δψm specific stain Rhodamine 123 (Rh-123) (10 µg/mL) for 30 min at 37 ^{0}C. The cells were then washed twice with methanol to remove the excess stain, washed again

with PBS, and analyzed for changes in Δψm using fluorescence microscope with an excitation and emission wavelengths of 505 nm.

2.10. Western blotting analysis

Crocin conjugated PEG- SeNPs treated cells were washed in PBS and lysed in 100 µL of buffer containing 50 mM Tris–HCl (pH 8.0), 150 mM NaCl, 1% Triton X-100, 1 mM phenylmethylsulfonyl fluoride, 10 µg/mL pepstatin, and 10 µg/mL leupeptin. After 20 min, extracts were centrifuged at 12,000 rpm for 10 min at 4^0C and supernatantswere stored at −80 ^{0}C until further use. Proteins (30µg/lane) were separated using 10% SDS-PAGE, and then transferred to polyvinylidene difluoride (PVDF) membranes. Afterwards, the membranes were blocked in TBST solution containing 5% (w/v) non-fat milk for 2 h, followed by overnight incubation at 4^0C with primary antibodies such as bax, bcl-2, caspase 9 and 3 and cytochrome c. β-actin was used as an internal control. After being washed with TBST buffer, the membranes were incubated for 1 h with the secondary antibody, horseradish peroxidase-conjugated goat anti-rabbit IgG. Antibody-bound proteins were detected using enhanced chemiluminescence reagents. Blots were washed with washing buffer and incubated with secondary antibodies conjugated with horseradish peroxidase for 1 h at room temperature.

2.11. Hemolytic assay

Ethylenediamine tetraacetic acid (EDTA)-stabilized human blood samples were freshly collected. A sample of whole blood (4 mL) was added to phosphate-buffered saline (8mL, PBS: pH 7.4). The Red blood cells (RBCs) were isolated by centrifugation at 10016 g for 5 min and further washed five times with sterile PBS solution. Following the last wash, the RBCs were diluted with PBS (40 mL). Then diluted RBC suspension (0.2 mL) was added to crocin conjugated PEG- SeNPs solutions at systematically varied concentrations and mixed by

vortexing. All the sample tubes were kept in static condition at room temperature for 3 h. Finally, the mixtures were centrifuged at 10016 *g* for 3 min, and 100 μL of supernatant of all samples was taken, and its absorbance was recorded on a spectrophotometer (Shimadzu UV–*vis* Spectrophotometer) at 545 nm. The percentage hemolysis was calculated using the following relationship.

$$\text{Hemolysis \%} = \frac{\text{Sample absorbance} - \text{negative control}}{\text{Positive control} - \text{negative control}} \text{ X } 100$$

Herein, RBC incubation with deionized water and PBS were used as the positive and negative controls, respectively.

2.12. Assessment of anti-tumor activity *in vivo*

The anti-tumor efficiency of crocin conjugated PEG- SeNPs was assessed in tumor-induced mice. Briefly, the subcutaneous dorsa of male nude mice were inoculated with A549 cells (1 x10^7) in 100 mL of normal saline. When the volume of the xeno-graft tumor reached approximately 50-75 mm^3 the mice were randomly divided into 3 groups and a control group with six mice in each group. Crocin conjugated PEG- SeNPs at dosages of 3.0, 6.0 and 9.0 mg/kg/day was injected intravenously every 2 days, and the mice were then observed for 16 days. The tumor diameters were measured every 3 days interval for each group. The tumor volumes (V) and body weight were calculated using the formula V = [length x (width)2]/2. For the assessment of toxicity, organs such as, liver, kidney and lung were collected, fixed in 4% paraformaldehyde solution and made into 4mm sections which were stained with hematoxylin and eosin (H&E) and observed under a microscope.

2.13. Statistical analysis

All the measurements were made in triplicate and all values were expressed as the mean ± standard error. The results were subjected to an analysis by Student's t-test. The results were considered statistically significant if the p-value was ≤ 0.05.

2.14. Live subject statement

The authors state that all experiments were performed in compliance with the relevant laws and institutional guidelines (Animal Ethical Committee, Periyar University, Salem) and this work has been approved by the IAEC (Institutional Animal Ethical Committee) constituted as per the Rules and Regulations of Ministry of Animal Husbandry, Government of India. The authors also state that informed consent was obtained for any experimentation with human subjects and Animal Ethical Committee, Periyar University, Salem is committed to the protection and safety of human subjects involved in research.

3. Results and Discussion

3.1. Identification of active compound

The GC–MS spectrum revealed the presence of various compounds present in saffron extracts (Fig. 1). Sixteen major compounds from GC/MS results were listed along with their retention indices and molecular weight (Table 1). The qualitative analysis of crocin was further confirmed with the assistance of HPLC. Chromatogram of high-performance liquid chromatographic analysis of commercially available crocin (used as standard) and crocin isolated from saffron extract were shown in (Fig. 2). Chromatogram of crocin isolated from saffron extract (Fig. 2b) showed peaks between 14 – 18 minutes consistent with the standard crocin [51] (Fig. 2a). The purity of crocin was 96 %.

3.2. Preparation and characterization of NPs

To validate the synthesis of PEG- SeNPs, UV-visible spectroscopy was performed (Fig. 3). The spectrum of PEG- SeNPs exhibited absorption maxima at 395 nm. Similar absorption maxima were observed for SeNPs synthesized using lemon leaf extract.[52] In addition previous reports have shown that the SeNPs contribute to the absorption maximum at around 200–400 nm in the UV-visible spectra.[53] Besides the insert of Fig 3 represents change in color during the nanoparticles synthesis. Initially the colloidal solution appeared colorless but after reduction with PEG, it turned to red color. This color change may be due to the surface plasma resonance (SPR) with a broad peak. Similar color chances were noted by Estevez *et al*.[54] during the formation of chitosan-stabilized selenium nanoparticles and Zheng *et al*.[55] during the formation of polyamidoamine-modified selenium nanoparticles. Thus color change from colorless selenious acid to red color (SeNPs), having absorption maximum (λmax) at 390 nm clearly indicates the formation of SeNPs using PEG. Further the conjugation of crocin onto the NPs was confirmed by the appearance of additional peaks at 470 and 475nm related to crocin.[56] These results support the successful conjugation of crocin to PEG-SeNPs.

3.2.1. TEM, DLS and zeta potential

The morphology and size of the nanoparticles were characterized using TEM and DLS. The micrographs of PEG- SeNPs and crocin conjugated PEG- SeNPs are shown in Fig. 4. The nanoparticles were dispersible and spherical in shape. The observed size of PEG- SeNPs (Fig. 4a) ranged approximately between 25-35 nm and those of crocin conjugated PEG- SeNPs (Fig. 4b) presented a slightly larger size of approximately 40-50 nm. The hydrodynamic diameters of the prepared nanoparticles measured by DLS (Fig. 5), were 31 ± 3 nm (PDI = 0.127 ± 0.09) for PEG- SeNPs (Fig. 5a) and crocin conjugated PEG- SeNPs were 46 ± 1 nm (PDI = 0.214 ± 0.01)

(Fig. 5b). Crocin conjugated PEG- SeNPs had a larger size distribution compared to PEG- SeNPs possibly due to the presence of crocin, leading to the formation of bigger particles with larger polydispersity. Hence upon addition of crocin, the PEG- SeNPs increased in size which may be due to the conjugation of crocin to the NPs surface. Furthermore, NPs of diameters larger than 200 nm are readily scavenged nonspecifically by monocytes and the reticuloendothelial system.[57] It was reported that smaller particles tended to accumulate at the tumor sites because of the EPR effect [58] with greater internalization. [59] Crocin conjugated PEG- SeNPs are thus convenient to benefit from the EPR effect and ideal for targeting tumors. Stability of the nanoparticles is vital for biomedical applications. Surface zeta potential is closely related to the stability of NPs and the zeta potential values of the as prepared NPs are shown in Fig. 6. The zeta potential of both the formulated nanoparticles were negative and ranged about -18.6 ± 0.26 mV for PEG- SeNPs (Fig. 6a) and - 31.36± 0.652 mV for crocin conjugated PEG- SeNPs (Fig. 6b). It was reported that NPs with negatively charged surface showed a reduced plasma protein adsorption and low rate of nonspecific cellular uptake. [60, 61] Meanwhile, the charged NPs can repel one another to overcome the natural tendency of aggregation of NPs.[62] Thus, crocin conjugated PEG- SeNPs had enough dispersion stability in aqueous solution and favorable for accumulation in the tumor tissue by EPR effect.

3.2.2. FT-IR and NMR

FT-IR analysis was conducted to characterize the changes in chemical bonds that occurred during the formation of the crocin conjugated PEG- SeNPs. Fig. 7 shows the FT-IR spectra of PEG- SeNPs and crocin conjugated PEG- SeNPs. The FT-IR of PEG-SeNP spectrum showed characteristic bands of PEG functional groups, such as the bands appearing at 2874.2 cm^{-1} assigned to the –CH group [63] and the band at 1103.9 cm^{-1} assigned to the –C–O–C group [64]

These two characteristic bands appeared in the PEG-SeNP spectrum, provided clear evidence that PEG forms part of the nanocomposite**.** Fig. 6 shows in case of PEG-SeNPs, the band at 3415 cm^{-1} is assigned to O– H stretching (n) vibrations. The bands at 2974 cm^{-1} corresponding to C– H stretching vibrations, at 1103 cm^{-1} corresponding to C – O– C are observed in PEG-SeNPs, conform the attachment of PEG onto SeNPs. FT-IR was further extended to study the conjugation of crocin with PEG-SeNPs. The band at 3353 cm^{-1} is due to stretching vibration of O-H which indicates the presence of alcoholic groups in crocin. The presence of bands at 1232-1410 cm^{-1} are due to stretching vibration of ester (O=C-O-) groups which are due to constituents of alcohol groups found in crocin.

The NMR spectra depicted in Fig. 8 authenticate the presence of PEG-SeNPs. The respective chemical shifts peaks had been noticed at 9.61, 9.22, 3.61 and 3.34 ppm. The peak at 3.61 ppm is related to the principle proton peaks from PEG.[65] The incorporation of PEG in SeNPs was thus confirmed by observing the proton peaks from PEG (CH_2 at 3.61 ppm) in the PEG-SeNPs. Interestingly the crocin conjugated PEG- SeNPs accentuated the characteristic peaks at 9.65, 9.15, 3.50 and 3.36 ppm. The conjugation of crocin was confirmed by the appearance of principle peaks of crocin at 1.97, 2.40, 6.50 and 7.40 ppm.[66, 67] The Chemical shift timing may slightly be varied for a complex when it is structurally further modified with other compounds or molecules. Thus the data presented in the form of NMR spectra are more convening to confirm the nanoformulation of crocin conjugated PEG- SeNPs.

3.2.3. X-ray diffraction pattern

The crystal structure and the phase composition of crocin conjugated PEG- SeNPs were determined, using XRD techniques shown in Fig. 9. The XRD pattern suggests that the NPs were crystalline in nature. The diffraction peaks at 42.5 ^{0}, 57.8 ^{0}, and 62.3 ^{0} can be index to the crystal

planes of (1 1 1), (2 0 0) and (2 2 0) crystalline Se and well matched with the Standard JCPDS data (06-0362). The estimated average lattice constant was a = 4.363 A° which is consistent with the standard JCPDS data. The calculated grain size of crocin conjugated PEG- SeNPs was 44.7 nm.

3.2.4. Drug loading profile

To assess the feasibility of using PEG- SeNPs as drug carrier, we performed the loading efficiency of crocin onto PEG- SeNPs. The theoretical drug loading content was set at 10 wt%, and the results showed that the loading efficiency of crocin conjugated PEG- SeNPs was 8.77 wt%, implying that crocin was effectively conjugated onto the NPs. After crocin conjugation, PEG- SeNPs had a larger size (46 ± 1 nm) than crocin-free PEG- SeNPs (31 ± 3 nm).

3.3. pH-Mediated Release of crocin *in vitro*

The crocin release behavior from PEG-SeNPs was investigated in PBS solution at pH 7.4 and pH 5.3 to intimate the blood and lysosome environments *in vivo*. As shown in Fig. 10, the cumulative release amount of crocin from the nanoparticles at pH 5.3 was 47.0% within 1 h and 91.0% for 48 h, whereas the release rate at pH 7.4 was 11.6% in 1 h and finally reached 34.5% for 48 h. The results demonstrated that the release process at pH 7.4 was much slower than that at pH 5.3. One of possible reasons was the low solubility of crocin at pH 7.4 than that at pH 5.3. Thus PEG-SeNPs hold a promise as a pH-mediated release delivery vehicle for potential cancer therapy.

3.4. *In vitro* cytotoxicity

The *in vitro* cytotoxic effects of crocin conjugated PEG- SeNPs was evaluated against human lung cancer and normal cell lines by MTT assay (Fig 11). As shown in Fig 11a, crocin conjugated PEG- SeNPs inhibited A549 cell growth in a time- and dose-dependent manner.

Despite this potency, the toxicity of crocin conjugated PEG- SeNPs toward human normal cells (L-132) showed no appreciable deduction in cell viability in both 24 h and 48 h incubation, indicating that crocin conjugated PEG- SeNPs is highly biocompatible (Fig 11b). The IC_{50} concentration of crocin conjugated PEG- SeNPs was found to be 18.6 μM for 24 h and 7.9 μM for 48 h. These results indicate that, crocin conjugated PEG- SeNPs is efficient in reducing the toxicity in normal cells without sacrifice of its anticancer activity. Similar cytotoxicity was reported by Yanyu Huang *et al.* [37] in MCF-7 cells incubated with DOX-loaded Tf-conjugated SeNPs (Tf-SeNPs). More recently, Wen *et al.*[2] demonstrated that 5- fluorouracil-SeNPs (5FU-SeNPs) exhibited a broad spectrum inhibition against A375, MCF-7, HepG2, Colo201, and PC-3 cancer cells. Despite this potency, 5FU-SeNPs showed much lower cytotoxicity toward human normal cells (Hs68 human fibroblasts, HK-2 proximal tubular cells, and MCF-10A human mammary epithelial cells). Interestingly, MCF-10A cells were also used as a model to examine the effects of 5FU-SeNPs on normal breast cells as compared to human breast cancer cells (MCF-7 cells). The results of their study showed that 5FU-SeNPs exhibited lower cytotoxicity toward MCF-10A than MCF-7 cells. Consistently our results also showed no appreciable toxicity toward human normal cells (L-132) when compared to human lung cancer (A549). These suggest that, the effects of crocin conjugated PEG- SeNPs on the human cells are cell-type specific. This selectivity could be partly due to the different protein and gene expression profiles of different cells which resulted in activation of different intracellular signaling pathways after exposure to crocin conjugated PEG- SeNPs. Taken together, our results suggested that crocin conjugated PEG- SeNPs possess great selectivity between cancer and normal cells and displays potential application in cancer chemotherapy.

To understand the synergistic interaction between PEG-SeNPs and the conjugated crocin, the growth inhibition of crocin conjugated PEG- SeNPs were analyzed by isobologram examination. The IC_{50} values for crocin conjugated PEG- SeNPs, crocin and PEG- SeNPs, were found at 6.2, 153.0, and 243.9 μM, respectively (Fig.11c). The results of the isobologram analysis revealed that the growth inhibitory effects between crocin and PEG- SeNPs in the crocin conjugated PEG- SeNPs system was strongly synergistic, as evidenced by the location of the data point in the isobologram being far below the line defining an additive effect [37]. The combination index (CI) of the crocin conjugated PEG- SeNPs was found at 0.024, which further confirmed the strong synergistic effects between crocin and the PEG- SeNPs. Taken together, our results clearly demonstrate that the strategy to use a SeNP as a carrier of crocin could be a highly efficient way to enhance its anticancer efficacy.

3.5. AO/EtBr staining for detection of apoptotic cells

The induction of apoptosis, after the treatment with IC_{50} concentrations of crocin conjugated PEG- SeNPs for 24 and 48 h was assessed by fluorescence microscopy after staining with acridine orange/ethidium bromide (AO/EtBr). The images of untreated and crocin conjugated PEG- SeNPs treated A549 cells are presented in Fig. 12a (Upper panel). The fluorescence microscopic analysis demonstrated that untreated A549 cells were stained with a uniform green fluorescence. Because AO can penetrate the normal cell membrane, the cells without treatment were observed as green fluorescence. In contrast the apoptotic cells formed as a result of nuclear shrinkage, blebbing were observed as orange colored bodies due to their loss of membrane integrity when viewed under fluorescence microscope.[58]

3.6. HOECHST 33342 staining for nuclear apoptosis

The characterization of the cell death induced by crocin conjugated PEG- SeNPs was further examined with the help of fluorescent DNA binding agent, HOECHST 33342. HOECHST 33342 is known to form fluorescent complexes with natural double-stranded DNA and is useful to find out the apoptotic nuclei. As seen from the images in Fig. 12a (Middle panel) untreated A549 cells had normal morphology with intact round nucleus emitting a weak fluorescence. However, cells treated with crocin conjugated PEG- SeNPs showed apoptotic nuclei, identified by reduced nuclear size, condensed chromatin gathering at the periphery of the nuclear membrane and a total fragmented morphology of nuclear bodies. Shanyuan Zheng *et al.*[48] explained the apoptosis of PEG-SeNPs treated HepG2 cells by means of similar morphological characteristics such as DNA fragmentation and nuclear condensation using staining techniques. Therefore, the anti-proliferation effect of crocin conjugated PEG- SeNPs would be associated with their potential to induce apoptosis in A549 cancer cells.

3.7. Analysis of mitochondrial membrane potential (Δψm) by Rhodamine 123 staining

The mitochondrial membrane potential (Δψm) loss of cancer cells was analyzed using the dye, Rh-123 [Fig. 12a (Lower panel)]. As can be seen from the image, a decrease in mean fluorescence intensity was observed following the treatment of cells with crocin conjugated PEG- SeNPs. The fluorescence images demonstrated the loss of mitochondrial membrane potential (Δψm) due to mitochondrial membrane depolarization, which was considered to be an initial and irreversible step of apoptosis.[68] The data indicated that the induction of apoptosis in cells by crocin conjugated PEG- SeNPs was accompanied by alterations in the mitochondrial membrane potential (Δψm). It was reported that mitochondria played an important role in an intrinsic apoptotic pathway by releasing cytochrome c, leading to the activation of the caspase

cascade.[69] The results demonstrated that crocin conjugated PEG- SeNPs could disrupt the functions of mitochondria at the early stages of apoptosis, subsequently coordinate caspase 3 activation through the cleavage of caspases by the release of cytochrome c. Fig. 12b shows that the total number of apoptotic cells increases when the incubation time increases.

3.8. Effect of crocin conjugated PEG-SeNPs on markers of intrinsic apoptotic gene expression

Apoptotic signaling pathway regulated by a complex network of molecules, involves the expression changes of distinct apoptotic proteins.[70] To elucidate the apoptotic pathways activated by crocin conjugated PEG- SeNPs, Western blot analyses were carried out to measure the expression of mitochondrial mediated apoptotic genes. It has been reported that bcl-2 members (e.g., bcl-2) protect against multiple signals that lead to cell death whereas bax members (e.g., bax,) induce apoptosis. [71,72,73] Previous studies demonstrated that down regulation of anti-apoptotic protein Bcl-2 leads to release of cytochrome c from the mitochondria to cytosol, which is an essential step in the induction of apoptosis. Cytochrome c release from mitochondria to cytosol in turn leads to the activation of the caspase cascade such as caspase-3 and 9 which is critical in executing apoptosis, as it is either partially or totally responsible for the proteolytic cleavage of many key proteins. [58] Thus it is remarkable to speculate the analysis of Bax, Bcl-2, cytochrome c, and caspases-3 and 9 gene expressions. The results (Fig. 13) revealed a significant decrease in the expression of Bcl-2 and with a significant increase in the expression of Bax, cytosolic cytochrome c and caspase-3 in cells treated with crocin conjugated PEG- SeNPs compared to untreated control. Thus, the induction of apoptosis was closely associated with the down-regulation of bcl-2, up-regulation of bax, loss of mitochondrial membrane potential, release of cytochrome c into cytosol, and subsequent activation of caspase cascades.

3.9. Blood Compatibility

Determination of hemolytic properties is one of the most common tests in studies of NPs interactions with blood components. [58] Hemoglobin release analysis (Fig. 14) shows the hemolytic activity of crocin conjugated PEG- SeNPs. Hemolysis of crocin conjugated PEG-SeNPs at all the tested concentrations were found to be <5 %. It has been reported that up to 5 % hemolysis is permissible for biomaterials. [74] The largest percentage hemolysis obtained was 0.68 ± 0.012% for crocin conjugated PEG- SeNPs at 9 mg/ mL. Since this is much lower than 5%, it indicates that crocin conjugated PEG- SeNPs are hemocompatible for drug delivery applications. Fig. 15a shows photographs of the hemolytic test on the nanoparticle samples. When water is added to RBCs, hemolysis takes place and the released hemoglobin emits red color. This serves as a positive control and represents 100 % hemolysis. RBCs incubated with PBS were used as negative controls and represents 0% hemolysis. The supernatant from crocin conjugated PEG-SeNPs at different concentrations is achromatic, and is comparable to that suspended in PBS. Thus, crocin conjugated PEG- SeNPs at the tested concentration exhibited no significant hemolysis. The cell morphology analysis (Fig. 15b) indicated that incubation of RBCs with 9 mg/ mL crocin conjugated PEG- SeNPs did not result in hemolysis or change in morphology of red blood cells when compared to control, thus implying the biocompatibility of the NPs. Yu-Shen Lin *et al*. [75] showed the influence of PEG surface coating on hemolytic activity of mesoporous silica nanoparticle (MS NPs). The authors report that contrary to bare MS NPs, no apparent hemolysis was observed for PEG-coated MS NPs after 3 h blood incubation. In our study, the absence of hemolysis maybe due to biocompatible polymer PEG coating which prevented the adhesion of both the NPs to red blood cell membrane. Thus this simple surface

modification stratagem is critical to ensure the safety of crocin conjugated PEG- SeNPs in biomedical applications.

3.10. *In vivo* anticancer activity of crocin conjugated PEG- SeNPs

In vivo therapeutic efficacy of crocin conjugated PEG- SeNPs is a crucial index for its future medical potential. Therefore, we treated A549 xenografts nude mice with different dosages of crocin conjugated PEG- SeNPs to examine its *in vivo* anticancer efficacy. At the end of the experiments, the mice were sacrificed and the tumor weight and tumor volume were measured (Fig 16). The results show that crocin conjugated PEG- SeNPs significantly inhibited the proliferation of A549 cells in a dose dependent manner, as represented by the decrease in tumor volume (Fig 16a) and tumor weight (Fig. 16b). Besides, no distinct reduction was observed in the body weight of nude mice, indicating the mineral side effect of PEG- SeNPs after crocin surface decoration (Fig. 16c). These results demonstrate the effective *in vivo* tumor suppressed capacity of crocin conjugated PEG- SeNPs. Previous studies demonstrated that Tf-SeNPs at similar dosages caused effective *in vivo* tumor suppression in MCF-7 xenografts nude.[36] Further, histological analysis of mice treated with normal saline, crocin conjugated PEG-SeNPs at different concentrations revealed no significant signal of damage from H&E stained organ slices including liver, kidney, and lung (Fig. 16d). Taken together, these findings all indicated that crocin conjugated PEG- SeNPs showed potential therapeutic effect *in vivo.*

4. Conclusion

Our present works provide a design of delivery system by using PEG-SeNPs as a carrier of crocin to achieve anticancer synergism. The studies on *in vitro* crocin release revealed that faster release of crocin has been observed under the acidic condition, which is exactly what we expect. Crocin thus could principally be distributed around tumor tissues with an acidic

microenvironment rather than in the normal section. Therefore, PEG-SeNPs hold a promise as a pH-mediated release delivery vehicle for potential cancer therapy. Crocin conjugated PEG-SeNPs showed perfect hemocompatibility and exhibited enhanced cytotoxicity toward A549 cells (human lung cancer cellines) through induction of apoptosis *via* mitochondria mediated pathway. Furthermore, crocin conjugated PEG- SeNPs significantly inhibits *in vivo* tumor growth in nude mice model. Taken together, our results suggest that the strategy to use the PEG-SeNPs as a carrier of crocin could be a highly efficient way to realize synergistic treatment of lung cancer. Furthermore, crocin conjugated PEG- SeNPs may be candidates for further evaluation as a chemotherapeutic agent for other human cancers.

Conflict of interest

No conflict of interest was reported by the author of this article

Acknowledgments

This research work was partially supported by UGC - Basic Science for Research (BSR) - RFSMS (Ref. G2/ 3142/ UGC – BSR – RFSMS / 2013) and DST-Nano-mission Project, Department of Science and Technology, Nano-mission division, New Delhi (Ref. SR/NM/NS-60/2010 dt. 08-07-2011). We thank the CeNSE Department, Indian Institute of Science (IISc), Bangalore, India, for helping with all the characterizations techniques.

References

1. R. Prasan and R. Bhandari, *JTCM.,* 2015, **5,** 81-87.
2. L. Wen, L. Xiaoling, W. Yum-Shing, Z. Wenjie, Z. Yibo, C. Wenqiang and C. Tianfeng, *ACS nano.,* 2012, **6,** 6578–6591.
3. W. Yuxia, Z .Xingbo, Z. Jin, X. Songqiang and W. Chaojie, J. *Med. Chem.*, 2012, **55,** 3502−3512

4. Z. Zipeng, T. X Wei, C. X Yen-Jun, T. Trever, Z. Weizhong, L. Xin, N. Gang, L. Gang, Lianchun, P. Zhengwei, C. Xiaoyuan and X. Jin, *ACS Nano.*, 2014, **8,** 6004–6013.
5. F. Alexis, E. Pridgen, L.K. Molnar and O. C. Farokhzad, *Mol. Pharmaceutics.,* 2008, **5,** 505–515.
6. S. K. Sneha and M.R. Theresa, *Bioconjugate Chem.,* 2011, **22**, 1879–1903
7. H. J. Maeda, *Controlled Release*., 2012, **164**, 138−144
8. L. Pan, Q. He, J .Liu, Y. Chen, M. Ma and L. Zhang, *J Am Chem Soc.,* 2012, **134,** 5722-735.
9. M. Bruchez Jr, M. Moronne, P. Gin, S. Weiss and A. P. Alivisatos, *Science.,* 1998, **281**, 2013-2016.
10. G. Tkachenko, H. Xie, D. Coleman, W. Glomm, J. Ryan and M. F. Anderson, *J Am Chem Soc.,* 2003,**125,** 4700-4711.
11. M. Liong, J. Lu, M. Kovochich, T. Xia, S. G. Ruehm and A. E. Nel, *ACS Nan*o., 2008, **2**, 889-896.
12. W. Liu, X. Li, Y. S. Wong, W. Zheng, Y. Zhang and W. Cao, *ACS Nano.,* 2012, **6,** 6578-91.
13. K.K. Vekariya, J. Kaur and K. Tikoo, *Nanomedicine.,* 2012, **8,** 1125-1132.
14. L. Kong, Q. Yuan, H. Zhu, Y. Li and Q. Guo, Wang, *Biomaterials.,* 2011, **32,** 6515-6522.
15. B. Yu, Y. Zhang, W. Zheng, C. Fan and T. Chen, *Inorg Chem.,* 2012, **5,** 8956-8963.
16. Y. Zhang, X. Li, Z. Huang, W. Zheng, C. Fan and T. Chen, *Nanomedicine.,* 2013, **9,** 74-84.
17. S. H. Park , J.Y. Choi , Y. H. Lee , J.T. Park , H. Song , *Chem Asian J.,* 2015, **10**, 1452-1456.

18. S. Yu, W. Zhang, W. Liu, W. Zhu, R. Guo, Y. Wang, D. Zhang , J. Wang, *Nanotechnology*., 2015, **26**, 145703- 145718.

19. J.T. Rotruck, A.L. Pope, H.E. Ganther, A.B. Swanson, D.G. Hafeman, W.G. Hoekstra, *Science.*, 1973, **179**, 588–590.

20. J. Zhang, H. Wanh, X. Yan, L. Zhang, *Life Sci.,* 2005, **76,** 1099–1109.

21. A. Navas-Acien, J. Bleys, E. Guallar, *Curr Opin Lipidol*., 2008, **19**, 43–49.

22. A. L. Ray, R. D. Semba, J. Walston, L. Ferrucci, A. R. Cappola, M.O. Ricks , Q. L. Xue, L. P. Fried, *J Nutr*., 2006, **136**, 172–176.

23. C.D.Thomson, *Eur J Clin Nutr*., 2004, **58**: 391–402.

24. N. V. Popova, *Cancer Lett.,* 2002, **179,** 39–42.

25. C. Redman, J. A. Scott, A.T. Baines, J .L. Basye, L. C. Clark, C. Calley, D. Roe, C. M. Payne and M. A. Nelson, *Cancer Lett.,* 1998, **125,** 103–110.

26. B. Prokopczyk, J. G. Rosa, D. Desai, S. Amin, O. S. Sohn, E. S. Fiala and K. El-Bayoumy, *Cancer Lett.*, 2000, **161,** 35–46.

27. S. Y. Zheng, X. L. Li, Y. B. Zhang, Q. Xie, Y. S. Wong, Z .W. J. Heng, T. F. Chen, Int. J. Nanomed., 2012, **7**, 3939–3949

28. C. H. Ramamurthy, K. S. Sampath, P. Arunkumar, M. S. Kumar, V. Sujatha, K. Premkumar, C. Thirunavukkarasu, *Bioprocess Biosyst. Eng.,* 2013, **36**, 1131–1139

29. T. F. Chen, Y. S. Wong, W. J. Zheng, Y. Bai , L. Huang, *Colloids Surf. B*., 2008, **67**, 26–31

30. H. Y. Luo, F. F. Wang, Y. Bai, T. F. Chen, W. J. Zheng, *Colloids Surf. B*., 2012, **94**, 304–308

31. K .S. Prasad, H. Patel, T. Patel, K. Patel, K. P. Selvaraj, *Colloids Surf. B.,* 2013, **103** 261–266

32. H. Hu, G. X. Li, L. Wang, J. Watts, G. F. Combs and J. Lu, *Cancer Res.,* 2008, **14,** 1150–1158.

33. S. Li, Y. Zhou, R. Wang, H. Zhang, Y. Dong and C. Ip, *Mol. Cancer Ther.,* 2007, **6,** 1031–1038.

34. H. Wang, J. Zhang and H. Yu, *Free Radic Biol Med.,* 2007, **42,** 1524–1533.

35. J. Zhang, X. Wang and T. Xu, *Toxicol Sci*., 2008, **101,** 22–31.

36. P.A. Tran, L. Sarin, R. H. Hurt and T.J. Webster, *Int J Nanomedicine*., 2010, **5,** 351–358.

37. Y. Huang, L He, W. Liu, C. Fan, W. Zheng, Y.S. Wong and T. Chen, *Biomaterials.,* 2013, **34,** 7106 - 7116.

38. H. H Aung, C. Z. Wang, M. Ni, A. Fishbein, S. R. Mehendale, J. T. Xie, C. Shoyama and C. S.Yuan, *Exp.Oncol.,* 2007, **29,** 175–180.

39. C.F. Lv, C. L. Luo, H. Y. Ji and P. Zhao, *China journal of Chinese materia medica.,* 2008, **33,** 1612–1617.

40. H. Hosseinzadeh, H. R. Sadeghnia, T. Ziaee and A. Danaee, *J. Pharm. Pharm. Sci.,* 2005, **8,** 387–393.

41. H. Hosseinzadeh, N. B. Noraei, *Phytother. Res.,* 2009, **23,** 768–774.

42. N. Pitsikas, A. Boultadakis, G. Georgiadou, P. A. Tarantilis and N. Sakellaridis, *Phytomedicine.,* 2008, **15,** 1135–1139.

43. T. Ochiai, H. Shimeno, K. Mishima, K. Iwasaki, M. Fujiwara, H. Tanaka, Y. Shoyama, A. Toda, R. Eyanagi and S. Soeda, *Biochim. Biophys. Acta*., 2007, **1770,** 578–584.

44. H. Hosseinzadeh, M. H. Modaghegh and Z. Saffari, *Evid. Based Complement. Alternat. Med.,* 2009, **6,** 343–350.

45. H. Hosseinzadeh, A. Abootorabi and H. R. Sadeghnia, *DNA Cell Biol.,* 2008, **27,** 657–664.

46. A. Talaei, M.H. Moghadam, S.A. Sajadi Tabassi , S.A. Mohajeri, *J Affect Disord*., 2015, 174, 51–56

47. S. A. Mohajeri, H. Hosseinzadeh, F. Keyhanfar and J. Aghamohammadian, *J. Sep. Sci.,* 2010, **33,** 2302–2309.

48. S. Zheng, X. Li, Y. Zhang, Q. Xie, Y.S. Wong, W. Zheng and T. Chen, *Int J Nanomedicine.,* 2012, **7,** 3939–3949.

49. W. Liu, X. Li, Y.S.Wong, W. Zheng, Y. Zhang and W. Cao, *ACS Nano.,* 2012, **6,** 6578 - 6591.

50. T. Chen and Y. S.Wong, *Biomed. Pharmacother.,* 2009, **63,** 105–113.

51. S. A. Mohajeri, H. Hosseinzadeh, F. Keyhanfar and J. Aghamohammadian, *J. Sep. Sci.,* 2010, **33,** 2302–2309.

52. K. S. Prasad, H. Patel, T, Patel, K. Patel and K. Selvaraj, *Colloids Surf. B.,* 2013, **103,** 261– 266

53. C. H. Ramamurthy, K. S. Sampath, P. Arunkumar, M. Suresh Kumar, V. Sujatha and K. Premkumar, C. *Bioprocess Biosyst Eng.,* 2013, **36,** 1131–1139.

54. H. Estevez, J. Carlos Garcia-Lidon, L. Luque-Garcia and C. Camara, *Colloids Surf. B.,* 2014, **122,** 184–193.

55. W. Zheng, C. Cao, Y. Liu, Q. Yu, C. Zheng, D. Sun, X. Ren and J. Liu, *Acta Biomater.,* 2014, http://dx.doi.org/10.1016/j.actbio.2014.08.035.

56. A. Rubio Moraga, O. Ahrazem, J. L. Rambla, A. Granell and L. Go´mez Go´mez, *PLoS ONE., 2013,* **8,** 71946.

57. D. C. Litzinger, A. M. J. Buiting, N. Rooijen and L. Huang, *Biochim. Biophys. Acta.,* 1994, **1190,** 99–107.

58. K. Shanthi, K. Vimala, D. Gopi and S. Kannan, *RSC Adv.,* 2015, **5,** 44998 –45014

59. C. Li, *Adv. Drug Delivery Rev.,* 2002, **54,** 695–713.

60. C. He, Y. Hu, L. Yin, C. Tang and C. Yin, *Biomaterials.,* 2010, **31,** 3657–3666.

61. F. Alexis, E. Pridgen, L. K. Molnar and O. C. Farokhzad, *Mol. Pharm.,* 2008, **5,** 505–515.

62. P. Aggarwal, J. B. Hall, C. B. McLeland, M. A. Dobrovolskaia and S. E. McNeil, *Adv. Drug Delivery Rev.,* 2009, **61,** 428–437.

63. H. Mu, X. Wang, P. H. Lin, Q. Yao and C. Chen, *Atherosclerosis.*, 2008, **201,** 67–75.

64. H. Petersen, P. M. Fechner and A. L. Martin, *Bioconjug Chem*., 2002, **13,** 845–854.

65. C. Zhang, L. Qi Zhao, Y. Feng Dong , X.Yan Zhang , J. Lin and Z. Chen, *Eur. J. Pharm. Biopharm.,* 2010, **76,** 10–16.

66. Z. Liang, M.Yanga, X. Xua, Z. Xiea, J. Huanga, X. Lia and D. Yanga, *Separ Sci Technol.*, 2014, **49,** 1427–1433.

67. K. Manolis, A. Assimiadis, Petros and M.G. Polissiou, *Appl Spectrosc.,* 1998, **52,** 519-522.

68. C Adrie, M. Bachelet, M. Vayssier-Taussat, F. Russo-Marie, I. Bouchaert, M. Adib-Conquy, J. M. Cavaillon, M. R. Pinsky, J.F. Dhainaut and B. S. Polla, *Am. J. Respir. Crit. Care Med.,* 2001, **164,** 389–395.

69. J. Gil, S. Almeida, C. R. Oliveira and A. C. Rego, *Free Radic Biol* Med*.,* 2003, **35,** 1500–1514.

70. K. Vimala, S. Sundarraj, M. Paulpandi and S. Kannan, *Process Biochem.,* 2014, **49,** 160-172

71. R. Vivek, V. Nipun Babu, R. Thangam, K.S. Subramanian and S. Kannan., *Colloids Surf. B.,* 2013, **111,** 117– 123.

72. M. O. Hengartner, *Nature.,* 2000, **407,** 770–776.

73. S. Y. Jeong and D. W. Seol, *BMB Reproduction.,* 2008, **41,** 11–22.

74. J. P. Singhal and A.R. Ray, *Biomaterial*s., 2002, **23,** 1139–1145.

75. Y. S. Lin and C. L. Haynes, *J. Am. Chem. Soc.,* 2010, **132,** 4834– 4842.

Figure Legends

Figure.1: GC-MS spectrum of saffron extract.

Figure.2: a) Chromatogram of HPLC analysis of commercially available crocin (used as standard), the insert shows the structure of crocin and b) crocin isolated from saffron extract.

Figure.3: UV-vis spectrum of PEG-SeNPs and crocin conjugated PEG- SeNPs. The insert shows a digital image of the color changes during the nanoparticles synthesis. Initially the colloidal solution appeared colorless but after reduction with PEG, it turned to red color.

Figure.4: FT-IR spectrum of PEG-SeNPs and crocin conjugated PEG-SeNPs.

Figure.5: NMR spectrum of PEG-SeNPs and crocin conjugated PEG-SeNPs

Figure.6: TEM micrographs: (a) PEG-SeNPs and (b) crocin conjugated PEGy-SeNPs. The particles were almost spherical in shape. The size of PEG-SeNP ranged approximately between 25–35 nm and crocin conjugated PEG-SeNPs presented a slightly large size of approximately 40 –50 nm.

Figure.7: The hydrodynamic diameters of (a) PEG-SeNPs and (b) Crocin conjugated PEG-SeNPs. PEG-SeNPs had an average size of 31 ± 3 nm (PDI = 0.127 ± 0.09) and crocin conjugated PEG-SeNPs had an average size of 46 ± 1 nm (PDI = 0.214 ± 0.01).

Figure.8: Surface zeta potential value of (a) PEG-SeNPs and (b) Crocin conjugated PEGy-SeNPs**.** The zeta potential of the nanoparticles were negative. PEG-SeNPs had zeta potential of -18.6 ± 0.26 mV and crocin conjugated PEGy-SeNPs had zeta potential of - 31.36± 0.652 mV.

Figure.9: XRD patterns of crocin conjugated PEG-SeNPs.

Figure.10: Cumulative crocin release (%) profile from PEG-SeNPs at 37 °C under pH conditions 5.3 and 7.4. The data points were average of at least three experiments. Bars represent the range over which the values were observed.

Figure.11: The cytotoxicities of crocin conjugated PEG-SeNPs against (a) A549 cells (b) Human normal lung epithelial cell lines L-132 as determined by MTT assay. Cells were treated with designated regimes for 24 h and 48 h. Data represent mean ± SD. *$p < 0.05$ was considered statistically significant. (c) Isobologram analysis of the anti proliferative effects of crocin and PEG-SeNPs on A549 cells.

Figure.12: (a) Fluorescent microscopic images of IC_{50} concentration of crocin conjugated PEG-SeNPs treated on A549 cells. ***Upper panel:*** Cells were stained with AO/EtBr staining to differentiate necrotic and apoptotic cells from one another. Note that untreated A549 cells were stained with a uniform green fluorescence. In contrast the apoptotic cells were observed as orange colored bodies whereas the necrotic cells were observed to be red in color. ***Middle panel:*** Cells were stained with Heochst stainning to visualize nuclear morphology. Note that untreated cells as control contained round nuclei with homogeneous chromatin and exhibited a less bright blue color. The cells treated with crocin conjugated PEGy-SeNPs showed chromatin condensation, reduction of nuclear size, nuclear fragmentation and the blue emission light in the apoptotic cells was much brighter. ***Lower panel:*** The mitochondrial membrane potential ($\Delta\psi m$) loss of cancer cells was analyzed using the dye, Rh-123. Crocin conjugated PEG- SeNPs could disrupt the functions of mitochondria at the early stages of apoptosis, subsequently coordinate caspase 3 activation through the cleavage of caspases by the release of cytochrome c. (b) Percentage of apoptotic cells were measured after A549 cells

were incubated with IC_{50} concentration of crocin conjugated PEGy-SeNPs. Data represent mean ± SD. *$p < 0.05$ was considered statistically significant.

Figure.13: Apoptosis induced by crocin conjugated PEG-SeNPs treated A549cells confirmed by western blot analysis of apoptotic related gene expressions. Expression of Bcl-2, cytochrome c, and caspases-3 after treatments with crocin conjugated PEG-SeNPs.

Figure.14: Percent hemolysis for crocin conjugated PEG-SeNPs at different concentrations for 3 h.

Figure.15: Hemolysis assay on crocin conjugated PEG-SeNPs (a) Photographs of hemolysis of RBCs incubated with different concentrations of crocin conjugated PEG-SeNPs. The presence of red hemoglobin in the supernatant indicates damaged RBCs. D.I. water (+) and PBS (-) were used as positive and negative control, respectively.(b) Microscopic image (magnification of 40×) of human RBC treated with crocin conjugated PEG-SeNPs (9 mg/mL). RBC without any treatment is used as control. No noticeable changes were observed for both the nanoparticles.

Figure.16: *In vivo* cancer therapy. (a) Tumor growth curves of four different groups of mice (4 mice per group) after treatments with different concentrations of crocin conjugated PEG-SeNPs showed varying degree of tumor suppression until the end of 16th day. The extent of tumor suppression is dose dependent and significantly higher in groups treated with a concentration of 9 mg/kg crocin conjugated PEG-SeNPs. (b) Effect of crocin conjugated PEG- SeNPs on Tumor weight. Crocin conjugated PEG- SeNPs showed dose dependent decrease in tumor weight. (c) Body weight of nude mice, no distinct reduction was observed. (d) Images show HE stained sections of liver, kidney and lung of the mice after treatment

with different concentrations of crocin conjugated PEG- SeNPs. No significant signals of damage were noticed.

Table Legend

Table 1: Phytochemical composition (%) of bioactive compound from stigma of saffron.

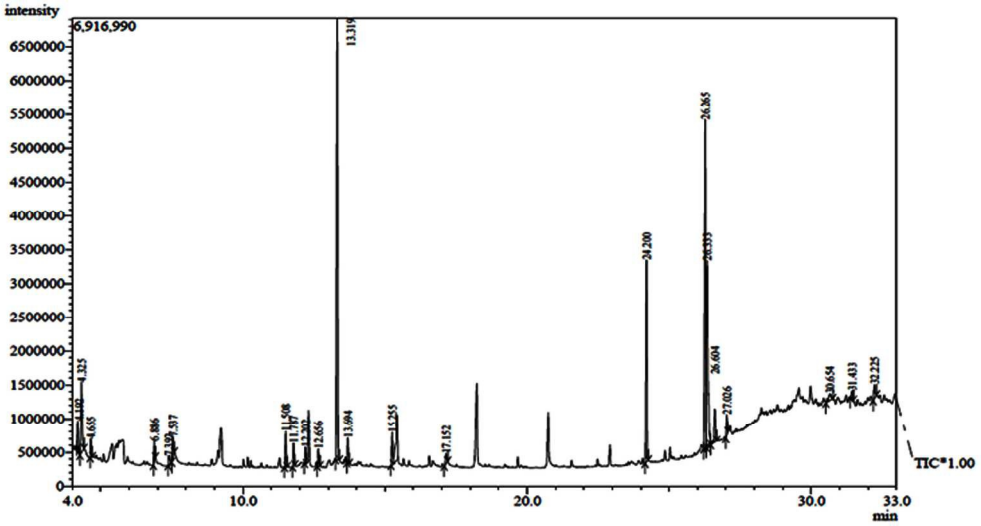

263x139mm (300 x 300 DPI)

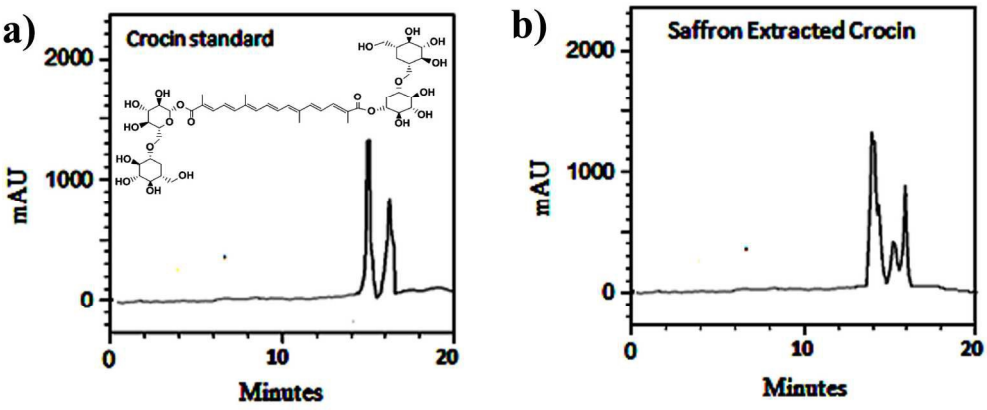

Fig 2
205x86mm (300 x 300 DPI)

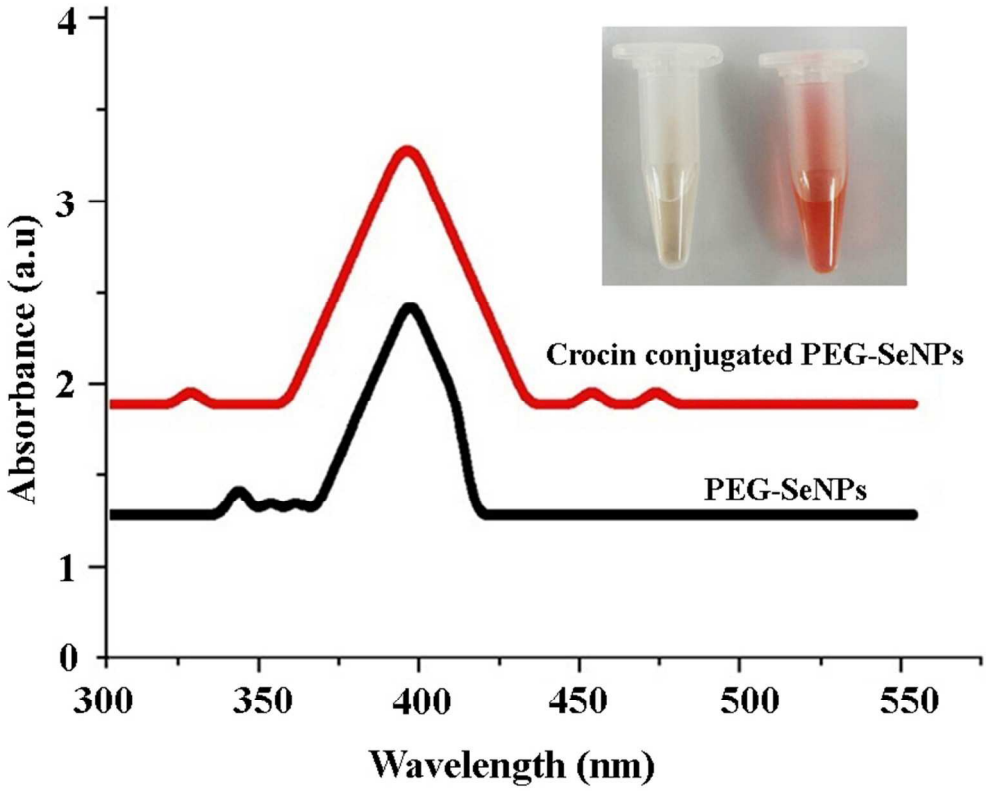

314x249mm (72 x 72 DPI)

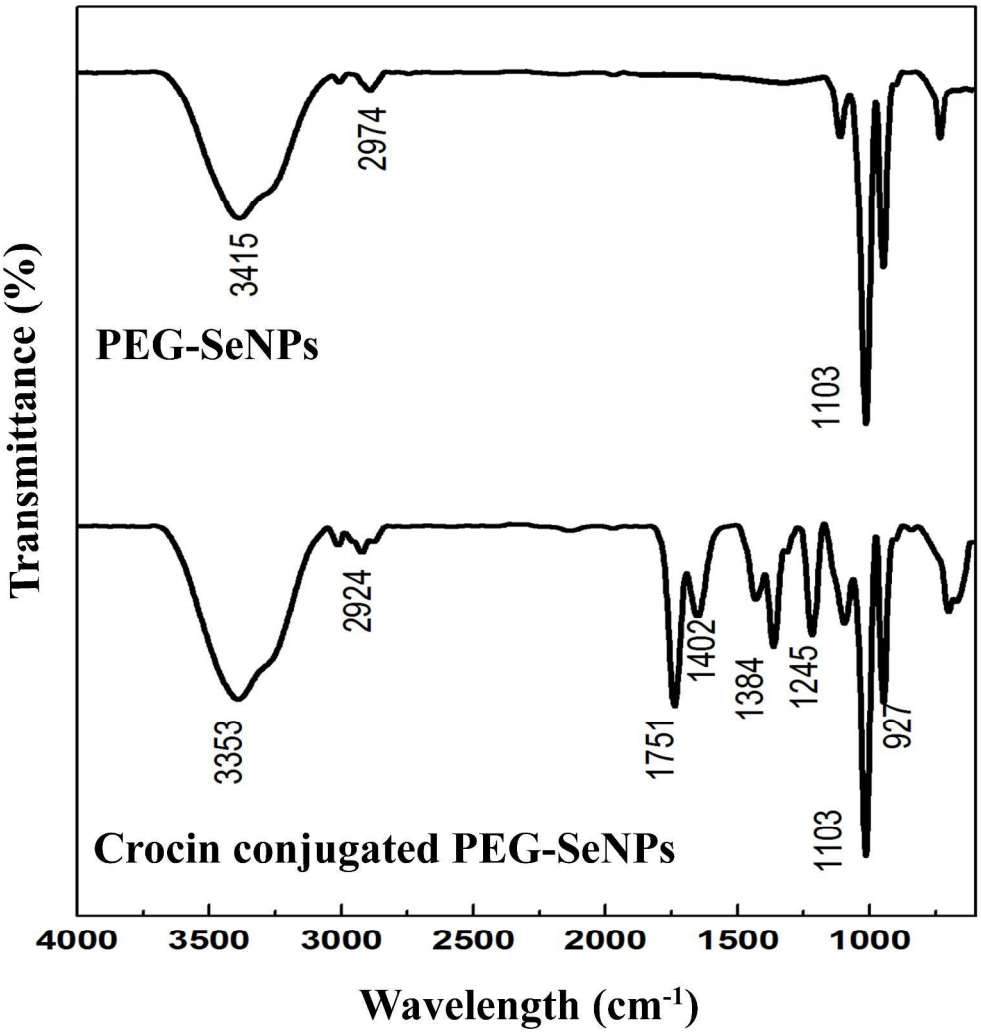

481x501mm (300 x 300 DPI)

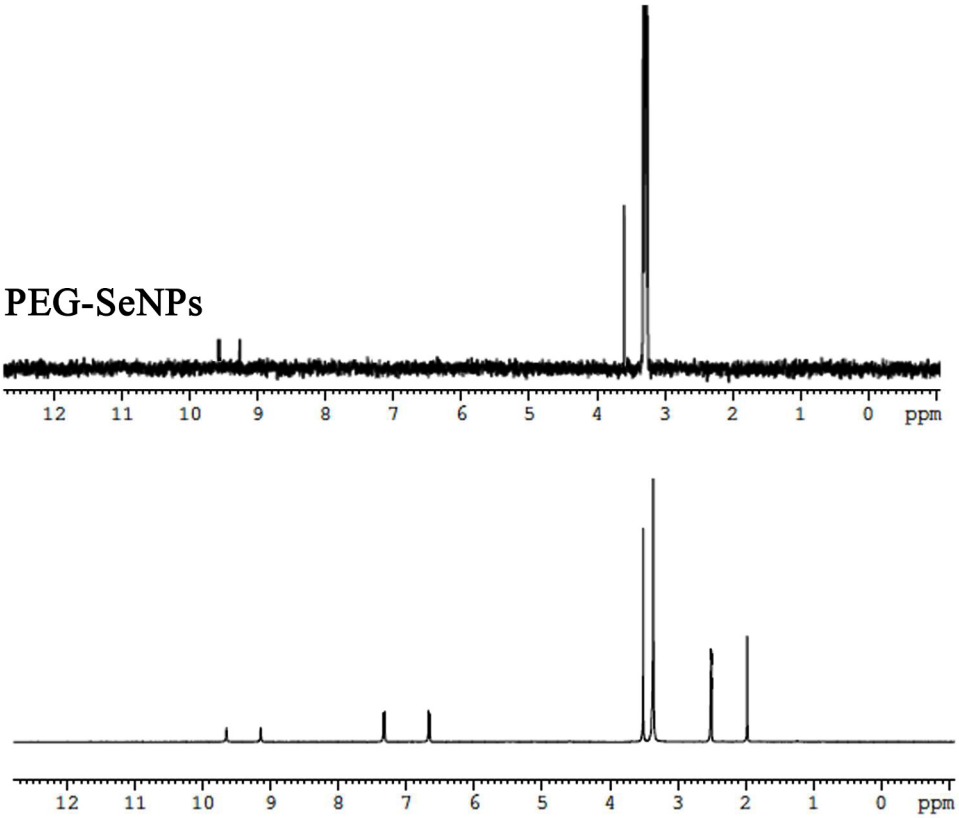

219x199mm (300 x 300 DPI)

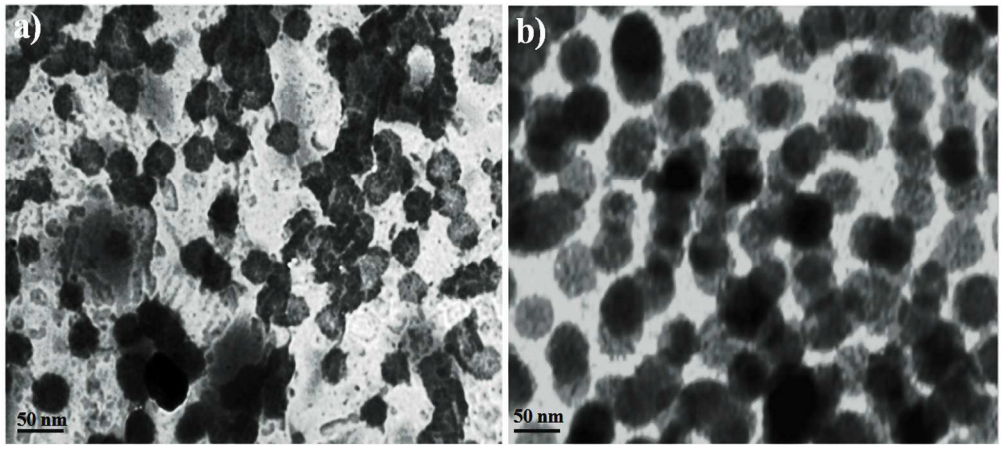

429x189mm (300 x 300 DPI)

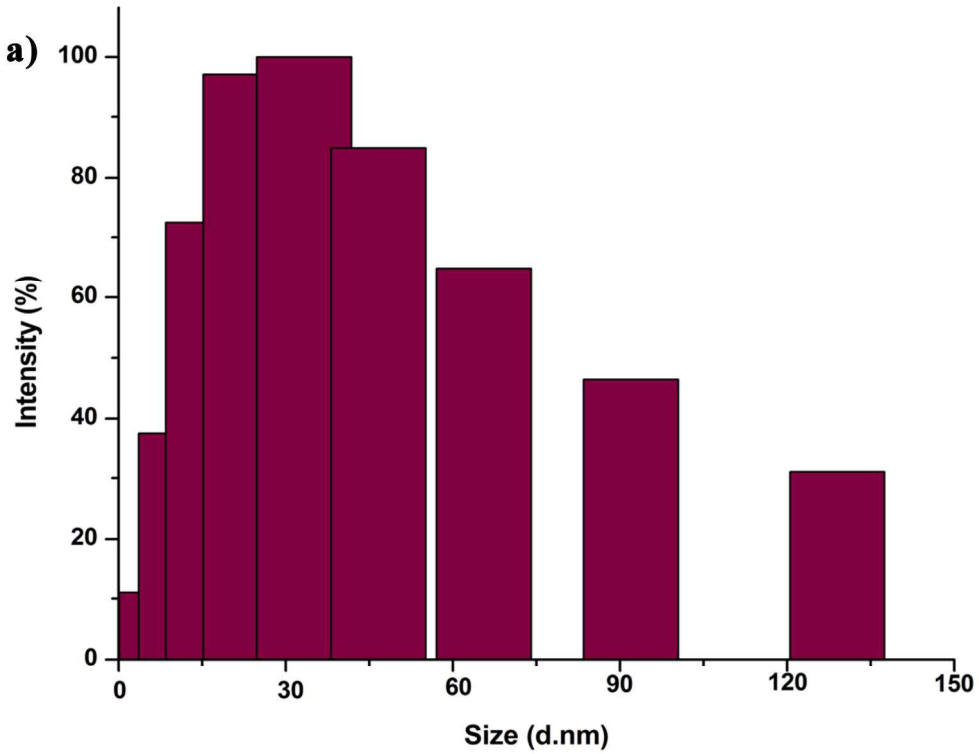

Fig 7a
271x208mm (300 x 300 DPI)

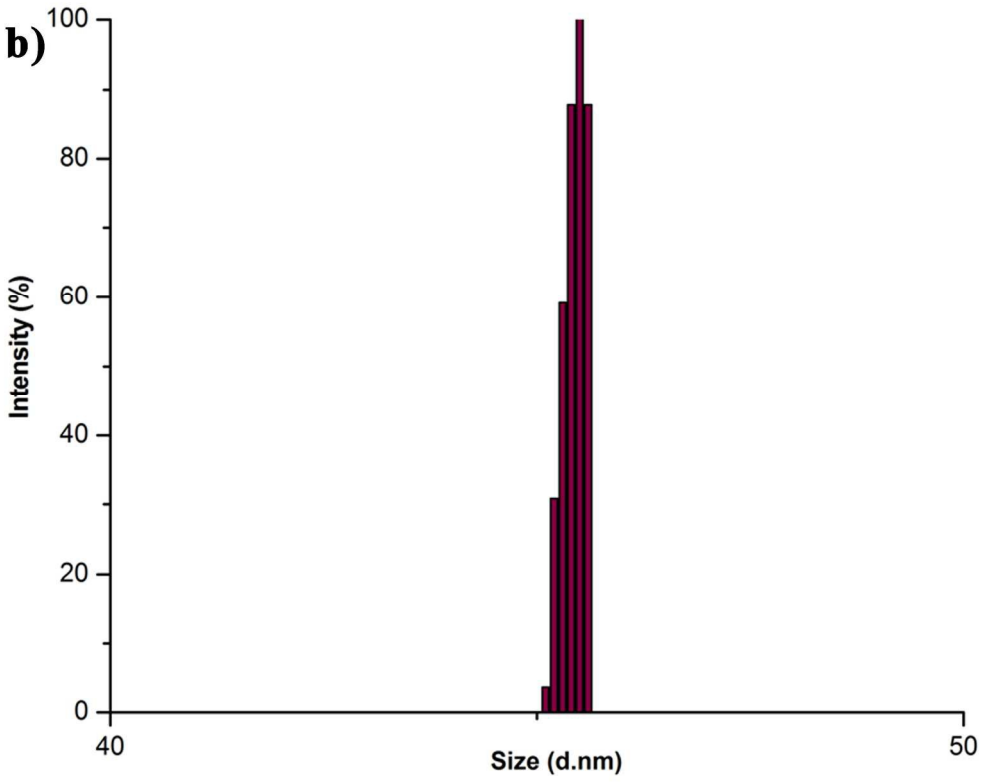

Fig 7b
239x193mm (300 x 300 DPI)

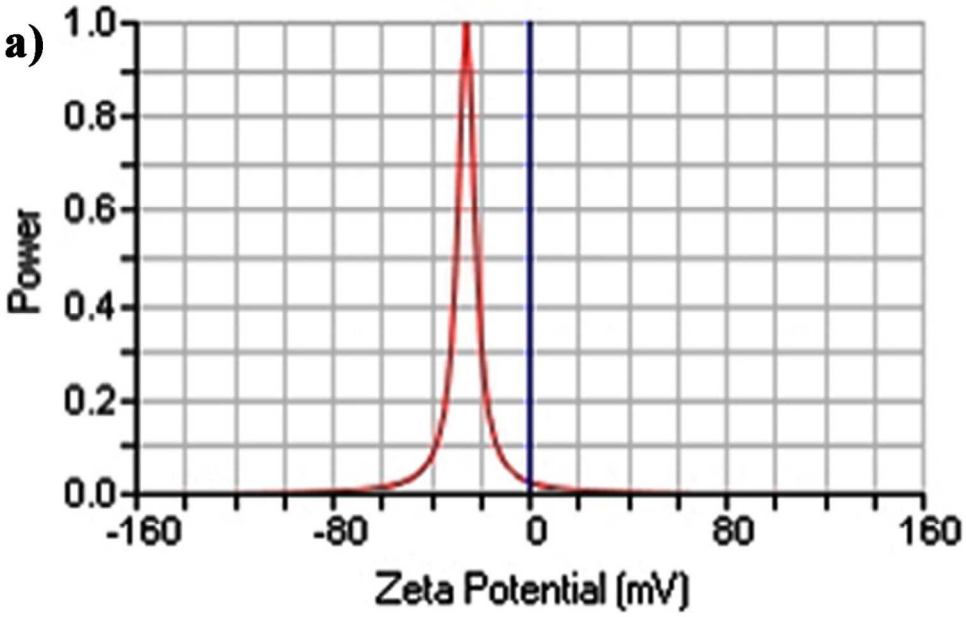

136x86mm (300 x 300 DPI)

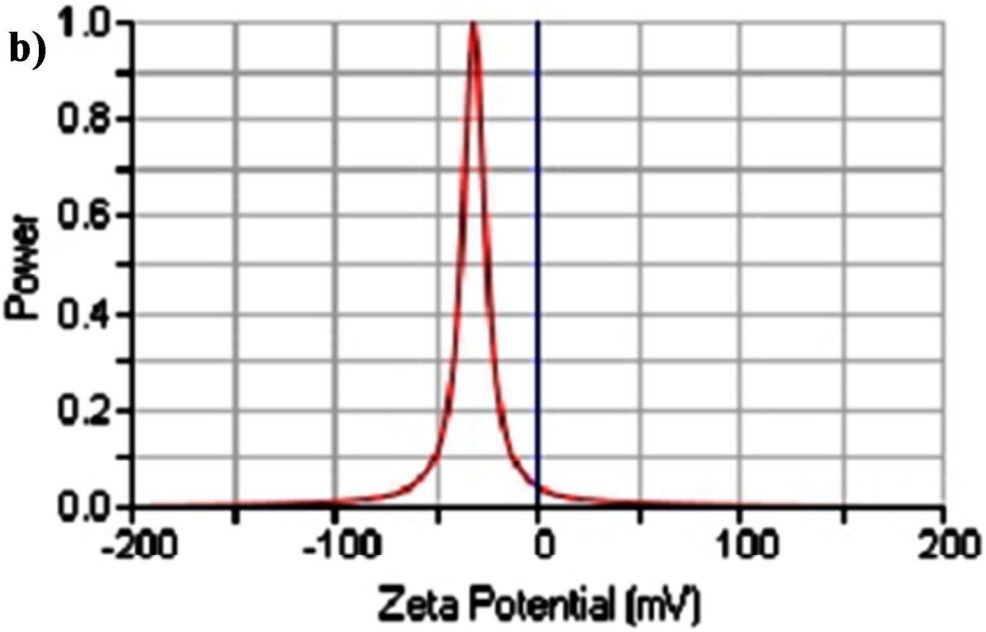

151x98mm (300 x 300 DPI)

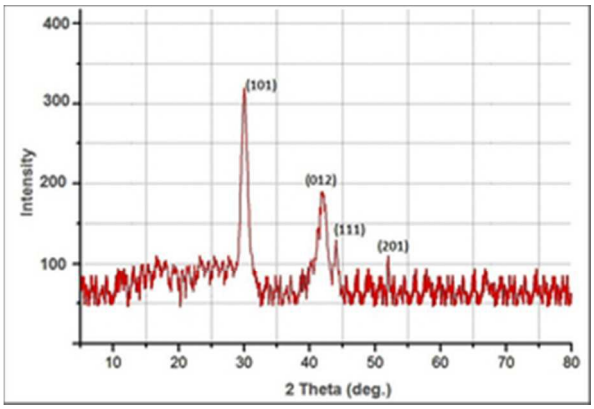

24x16mm (300 x 300 DPI)

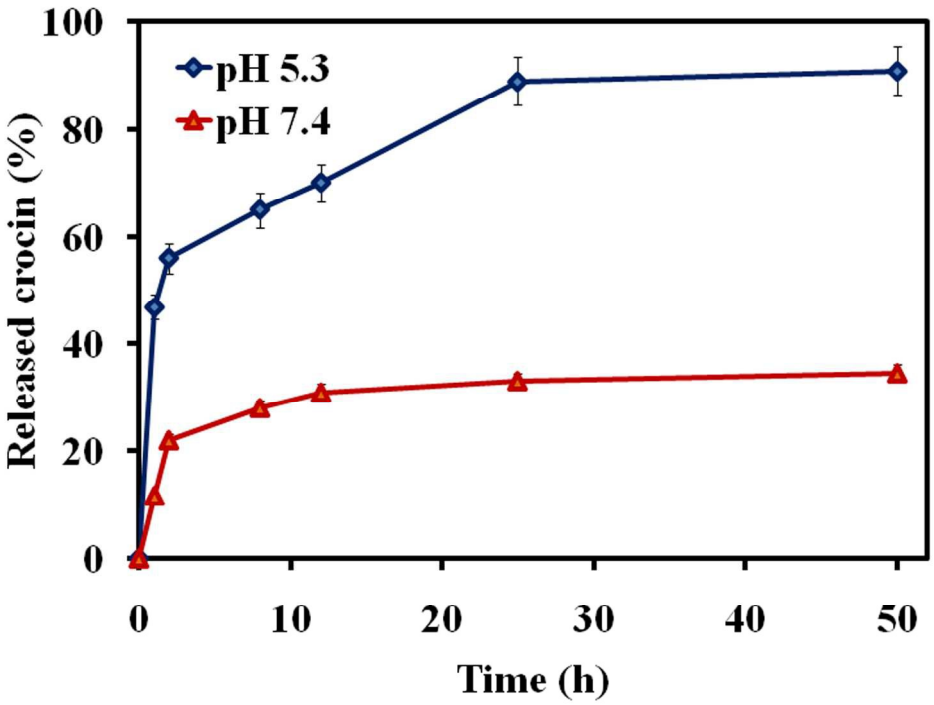

271x192mm (300 x 300 DPI)

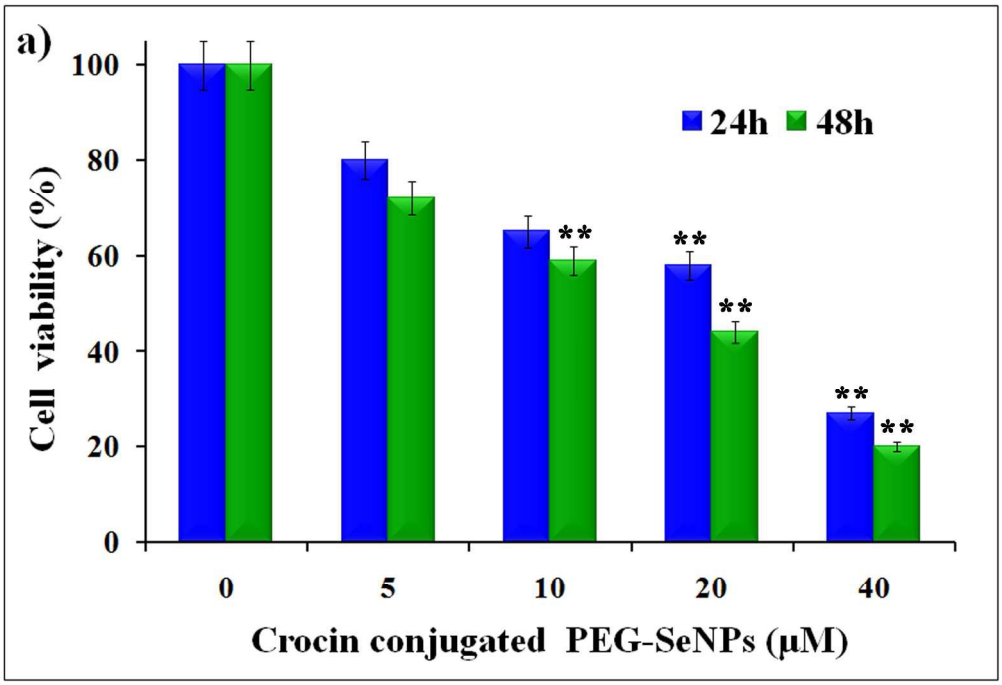

301x205mm (300 x 300 DPI)

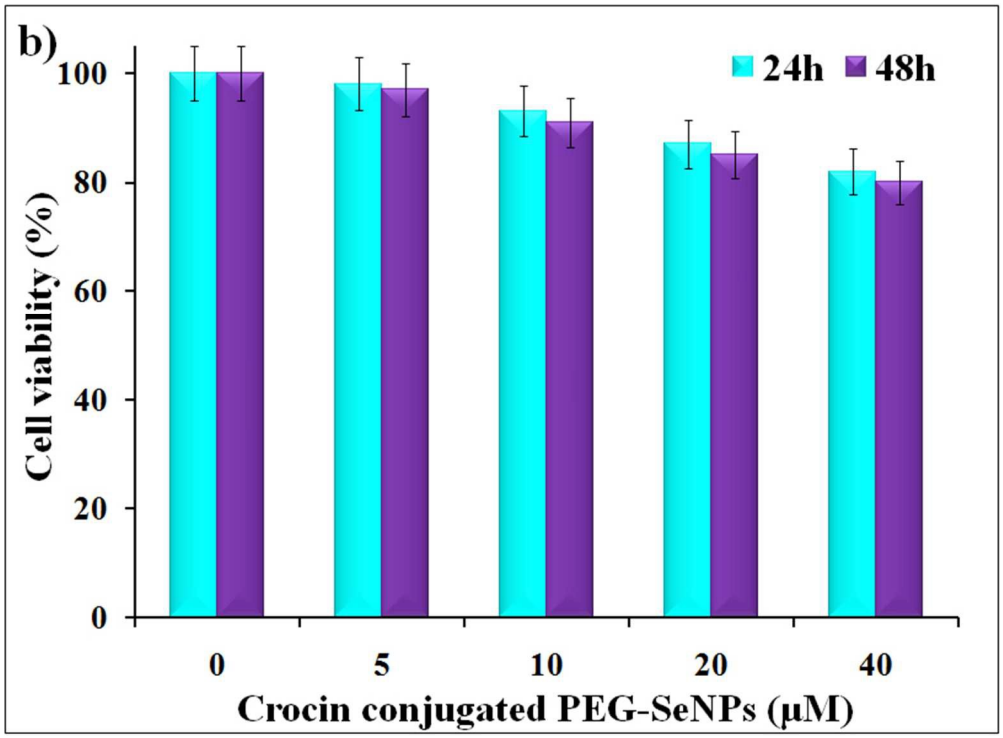

287x211mm (72 x 72 DPI)

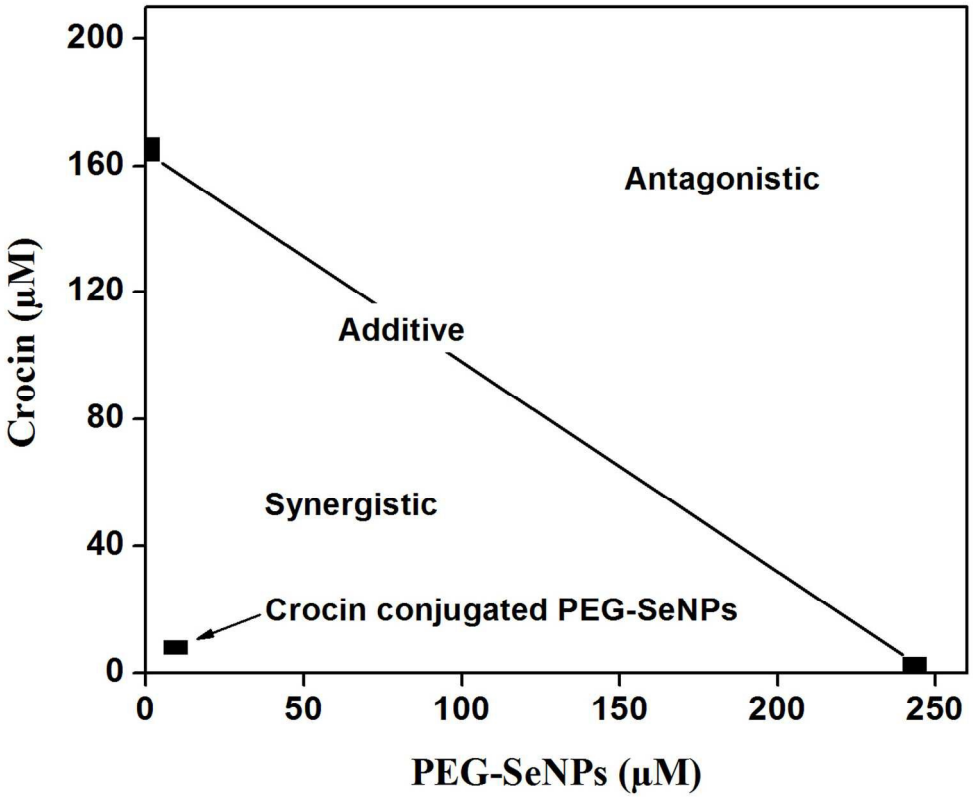

224x183mm (300 x 300 DPI)

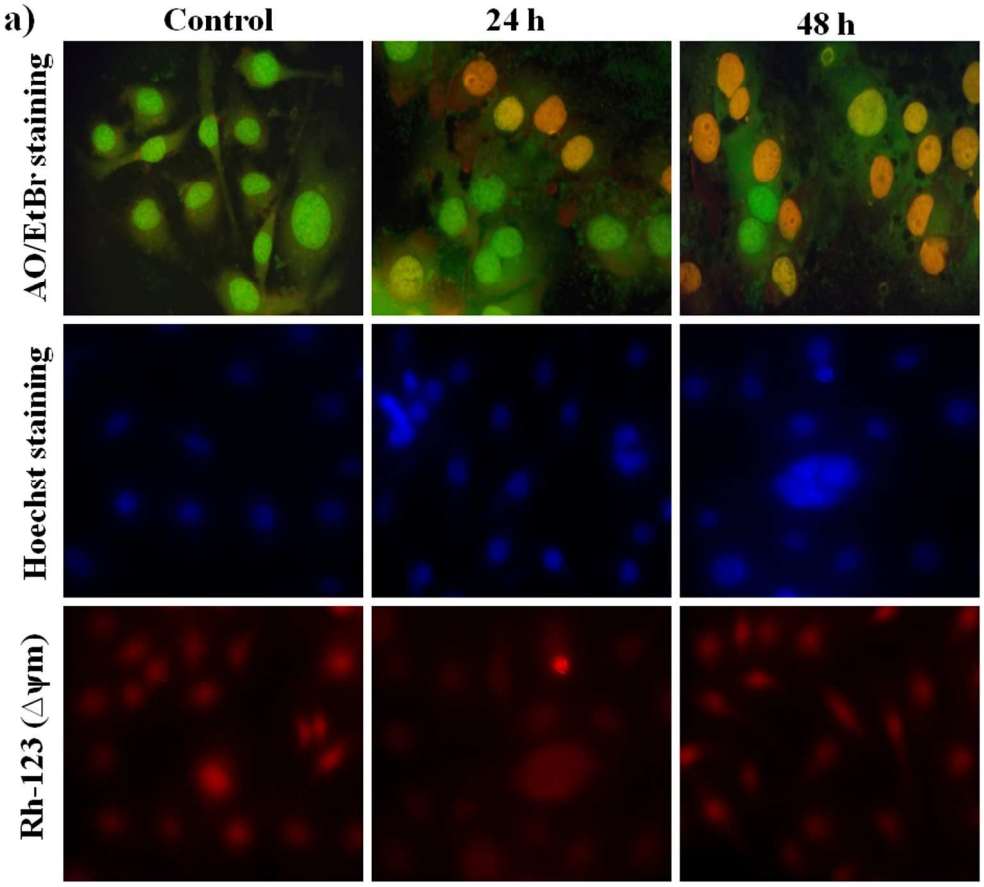

339x305mm (300 x 300 DPI)

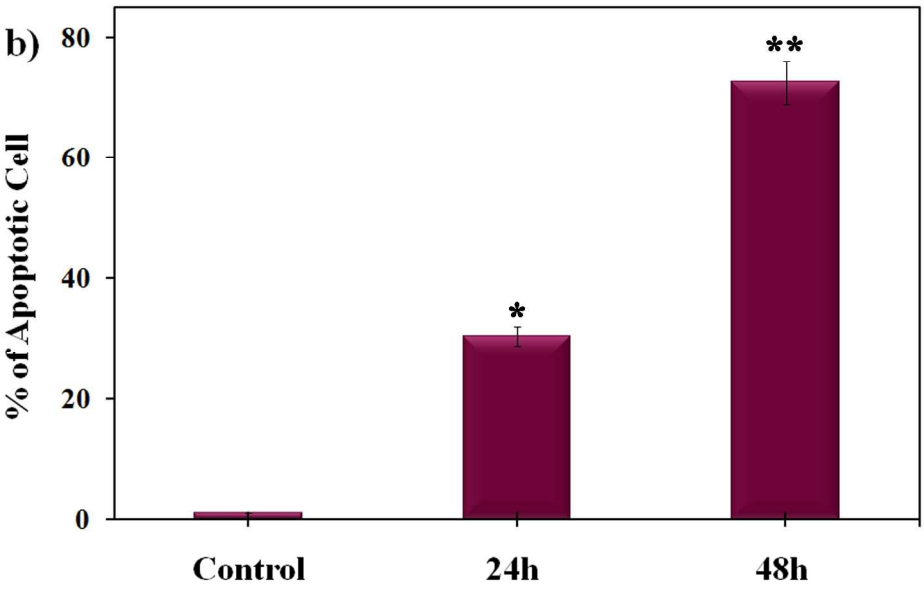

330x223mm (300 x 300 DPI)

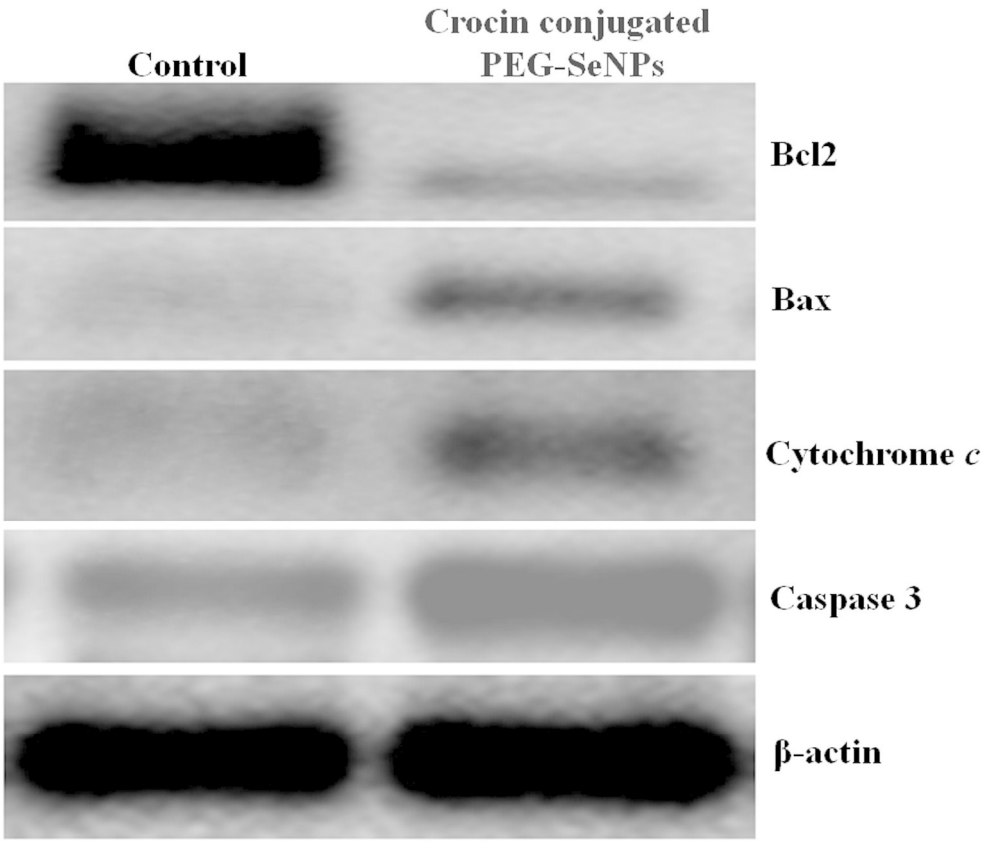

310x266mm (300 x 300 DPI)

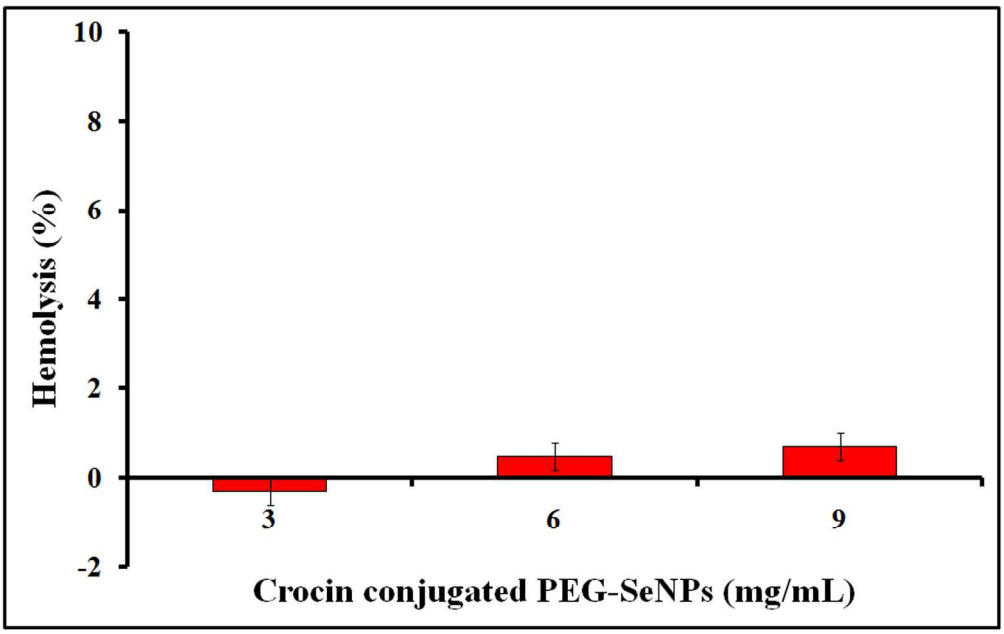

323x202mm (300 x 300 DPI)

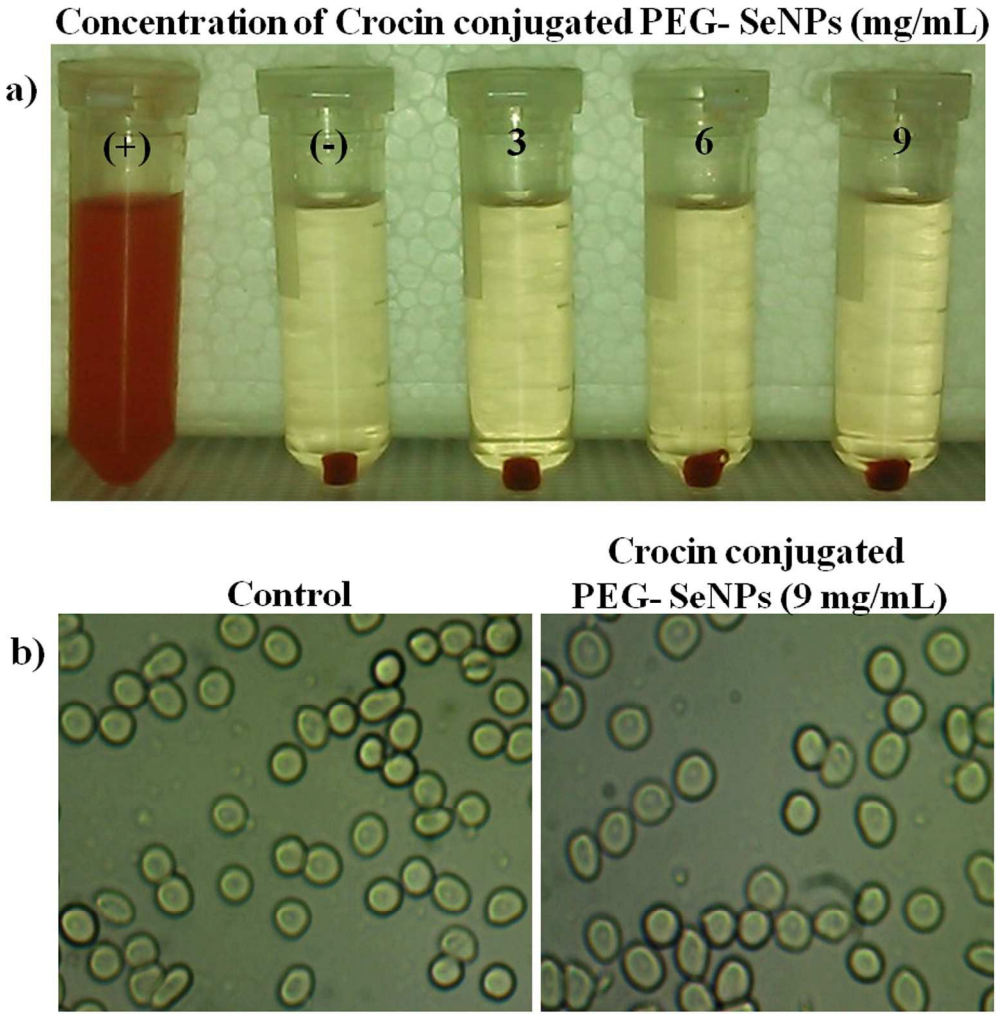

326x335mm (300 x 300 DPI)

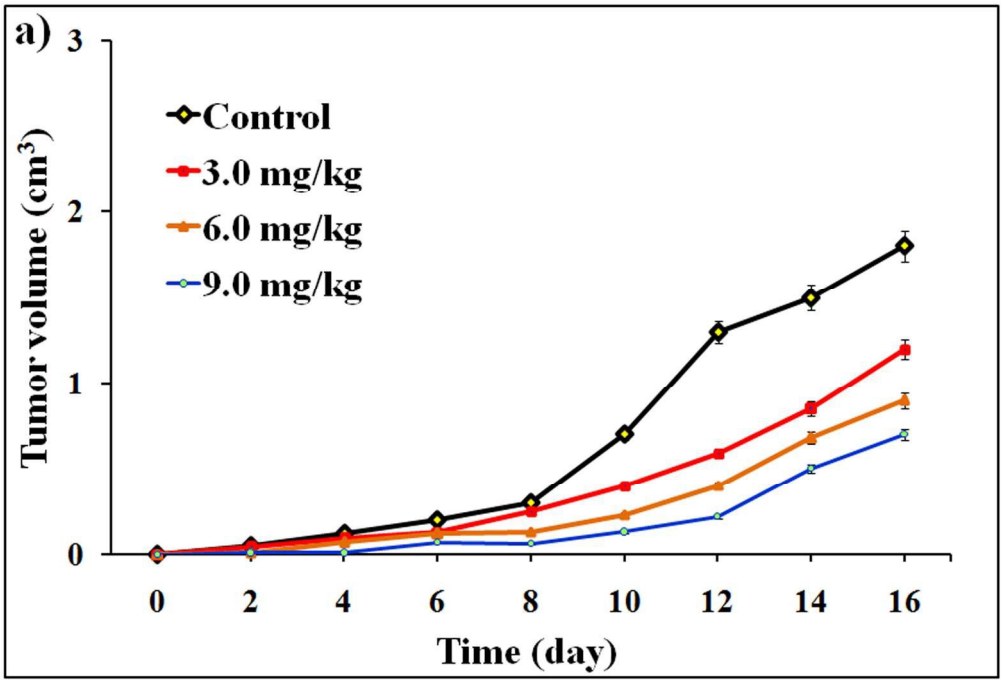

290x198mm (300 x 300 DPI)

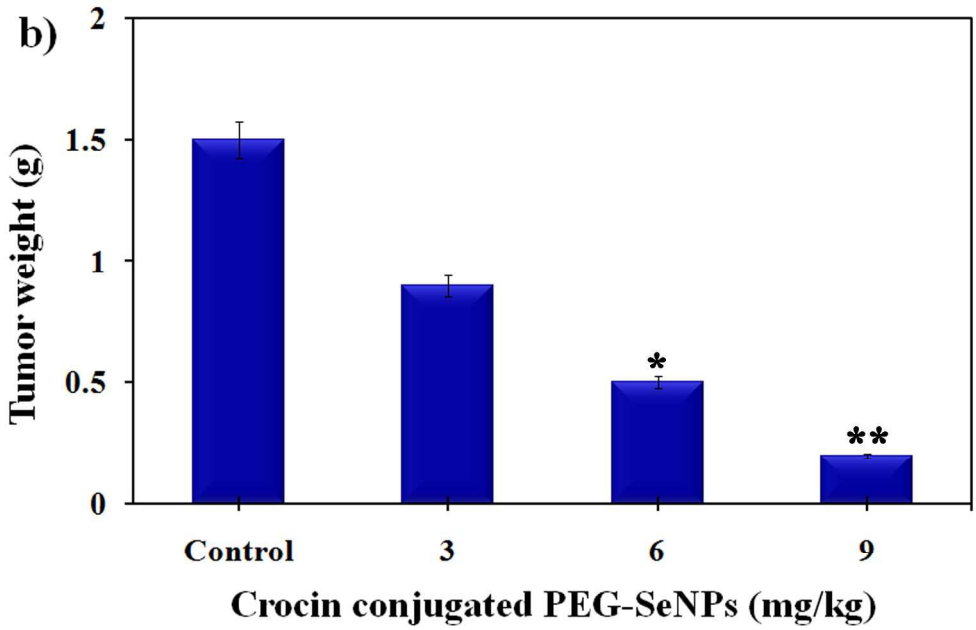

294x192mm (300 x 300 DPI)

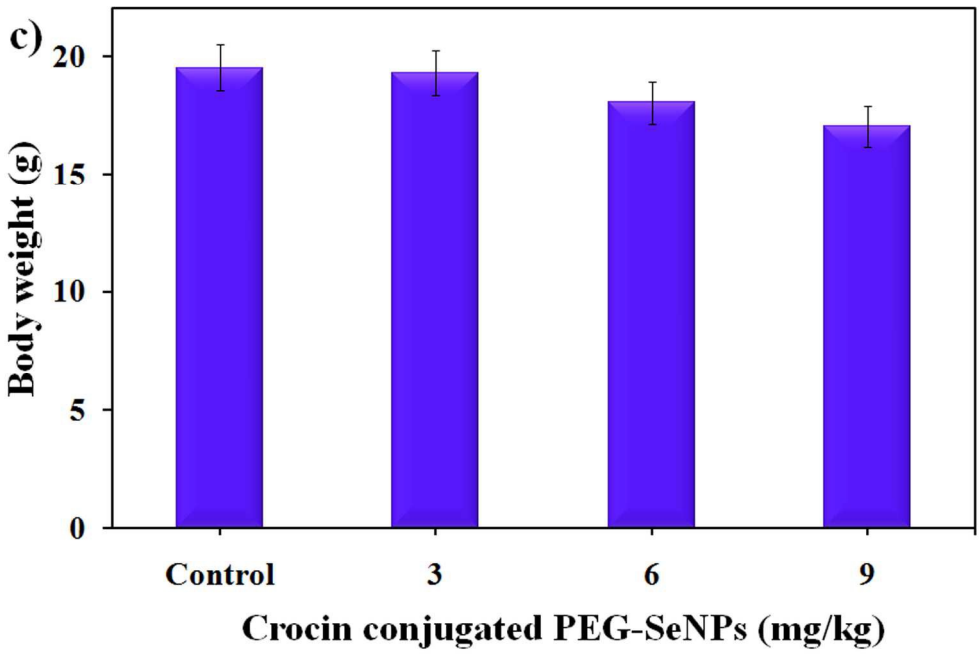

295x194mm (300 x 300 DPI)

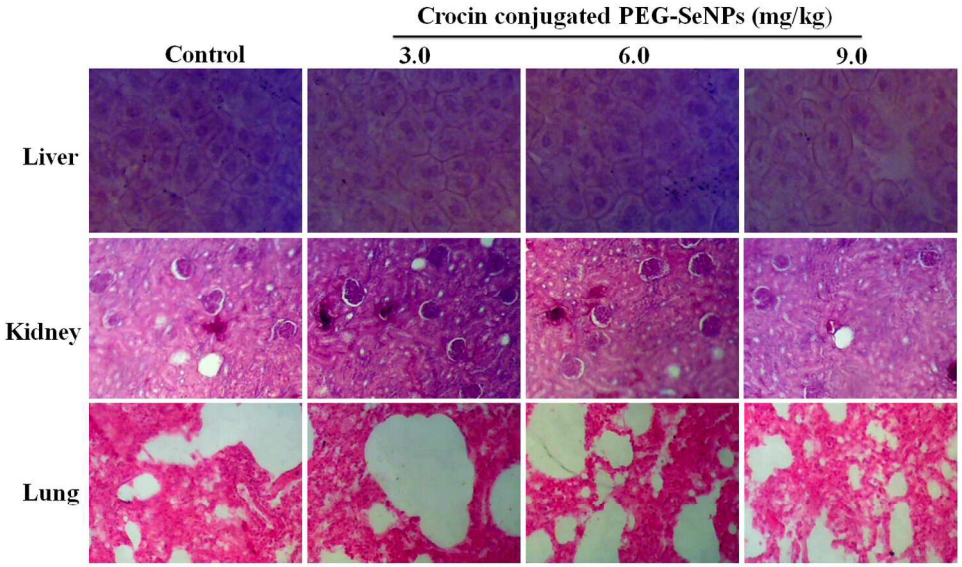

530x325mm (300 x 300 DPI)

Table. 1 Phytochemical composition (%) of bioactive compound from stigma of saffron

S.No	Compound	RT	Formula	M.W
1	Propyl Acetate	4.192	$C_5H_{10}O_2$	102.13
2	methyl (2R)-2-hydroxypropanoate	4.325	$C_4H_8O_3$	104.10
3	Ethylene Glycol	4.655	$C_2H_6O_2$	62.06
4	Methyleugenol	6.886	$C_{11}H_{14}O_2$	178.22
5	Methyl 2-methylbutyrate	7.392	$C_6H_{12}O_2$	116.15
6	Alloocimene	11.508	$C_{10}H_{16}$	136.23
7	Isophorone	11.787	$C_9H_{14}O$	138.20
8	Ketoisophorone	12.202	$C_9H_{12}O_2$	152.19
9	1,4-Cyclohexanedione, 2,2,6-trimethyl	12.656	$C_9H_{14}O_2$	154.20
10	Crocine	13.319	$C_{44}H_{64}O_{24}$	976.96
11	2,4-Cycloheptadien-1-one, 2-phenyl-	13.694	$C_{13}H_{12}O$	184.23
12	Mintlactone	15.255	$C_{10}H_{14}O_2$	166.21
13	Hexadecanoic acid, methyl ester	17.152	$C_{17}H_{34}O_2$	270.45
14	9,12-Octadecadienoic acid	26.265	$C_{18}H_{32}O_2$	280.44
15	8,11,14-Docosatrienoic acid	26.333	$C_{23}H_{40}O_2$	348.56
16	Octadecanoic acid, methyl ester	26.604	$C_{19}H_{38}O_2$	298.50
17	Ethyl linoleate	27.026	$C_{20}H_{36}O_2$	308.49
18	1-(4-Undecylphenyl) ethanone	30.654	$C_{19}H_{30}O$	274.44
19	2-fluoroadenine	32.225	$C_5H_4FN_5$	153.11

RT- Rate Time

M.W- Molecular Weight

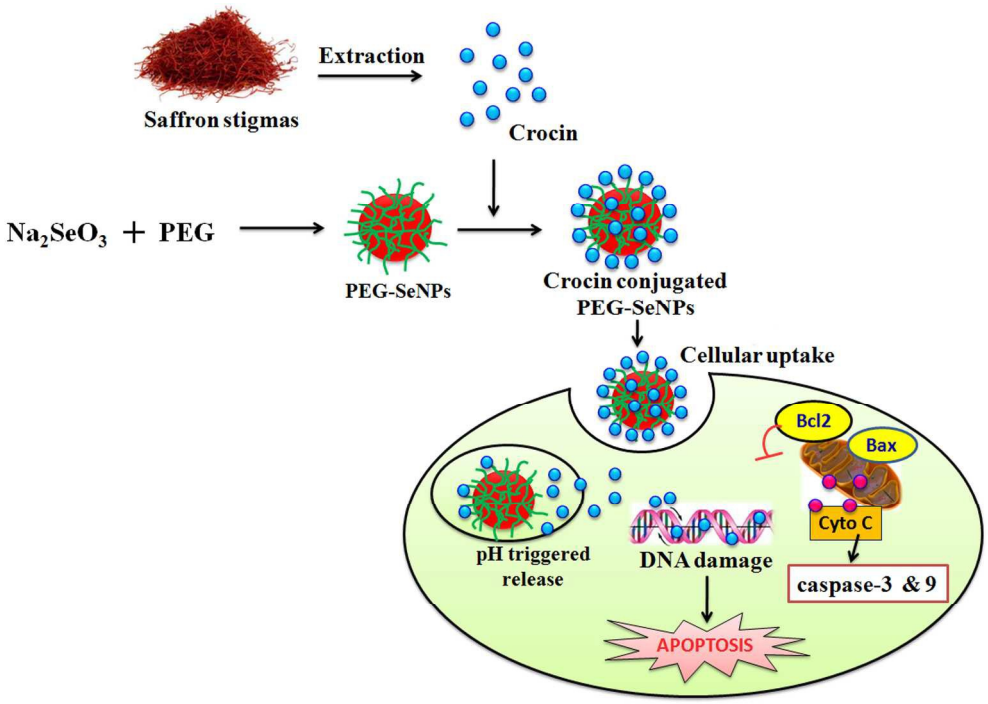

409x287mm (300 x 300 DPI)